NASA Contractor Report 177964

FINAL TECHNICAL REPORT

Small Business Innovative Research (SBIR)
Phase I

MICRO-RAMAN SPECTROSCOPY

THE ANALYSIS OF MICROMETER AND SUBMICROMETER ATMOSPHERIC AEROSOLS

Prepared for

Dr. Patrick McCormick
Dr. David Wood
National Aeronautics and Space Administration
Langley Research Center
Hampton, Virginia 23665

by

Stan M. Klainer
Fred P. Milanovich
ST&E Technical Services, Inc.
San Ramon, California 94583

Contract No. NAS1-17943
June 20, 1985

THE ANALYSIS OF MICROMETER AND SUBMICROMETER ATMOSPHERIC AEROSOLS USING MICRO-RAMAN SPECTROMETRIC TECHNIQUES

Summary

The objective of this research was to establish the feasibility of identifying and quantifying micron and submicron atmospheric aerosols using micro-Raman spectrometric techniques. The micro-Raman approach was chosen because: (i) it is non-destructive, (ii) it has both qualitative and quantitative chemical analytical capabilities, (iii) it provides both chemical and crystal structure information, and (iv) it is compatible with micro-size solid samples.

The research effort focused in three areas: (i) an evaluation and comparison of data from existing micro-Raman spectrometers, (ii) calculations specific to the non-destructive Raman analysis of micro particles, and (iii) the design of a micro-Raman spectrometer which would be compatible with NASA's requirements and which would be easy to operate. Micro-Raman spectra were obtained for aerosols of interest to NASA, i.e., carbon, sulfates, metal oxides, minerals, etc.

The research results have yielded the following information: (i) existing commercial micro-Ramon systems can analyze particles greater than 2 μm in diameter if high laser powers (greater than 10 mW) and long analysis times (greater than 1,000 s) are used, thus limiting the numbers and types of particles that can be analyzed because of potential photo and thermal degredation problems; (ii) the best micro-Raman spectrometer, at Lawrence Livermore National Laboratory, is capable of analyzing greater than 1 μm particles with approximately 1 mW of laser power in 300 s; (iii) the smallest particle analyzed was an approximately 0.8 μm particle with 1.4 mW of laser power and 300 s analysis time; (iv) the fastest micro-Raman analysis was 0.03 s for a 12 μm particle; (v) based on calculations and a preliminary new-generation instrument design, it should be possible to analyze a 0.3 μm particle in 1 s using 0.7 mW of laser power at 514.5 nm; and (vi) micro-Raman systems can be constructed which are not only fully automated, but which have the capability of preselecting the aerosols of interest as well.

This research will lead to a new generation micro-Raman system which can routinely analyze solids in the 0.3 μm diameter range and with potential for measuring aerosols of 0.1 μm in selected cases. This instrument will be the only system capable of doing non-destructive molecular analysis of submicron particles. Not only will it be useful for atmospheric research, but it will be of great benefit in materials, medical, pollution, catalysis, etc. studies.

TABLE OF CONTENTS

TABLES

FIGURES

1.0 Introduction

The collection and analysis of atmospheric aerosols is key to understanding upper atmosphere chemistry and perturbations which affect that chemistry. Much of the requisite information, however, is contained in micron and submicron size particles and these are not amenable to compound identification and quantification using existing methods of chemical analysis.

In order to fully utilize the information contained within a collected particle requires a non-destructive method of molecular analysis. Upper atmosphere reaction mechanisms can only be assessed if chemical compounds (and structures) can be identified. Elemental analysis cannot identify compounds, chemical transitions, crystal lattice deformations, etc. Whereas in simple systems possible molecular compounds can be inferred from stoichiometry or molecular fragments, in complex chemical systems, such as anticipated in upper atmosphere aerosols, the randomness of the situation makes "guess work" at best, risky.

In the present research, the feasibility of using micro-Raman spectrometric techniques for performing the required analysis has been evaluated. The results were exceptionally favorable and have led to the conclusion that micron and submicron particles can be analyzed using the micro-Raman approach. Furthermore, completely automatic analysis should be possible to 0.3 μm. Smaller particles should be analyzable, but here the skill of the operator begins to play an important role. No problems are anticipated with photo or thermal decomposition. Sample and impurity fluorescence will be the key source of background as they cannot be completely eliminated.

1.1 Background

Figure 1 is a diagrammatical representation of this research effort from its inception to an SBIR Phase II proposal. The project was conceived in

MICRO-RAMAN SPECTROMETER DEVELOPMENT

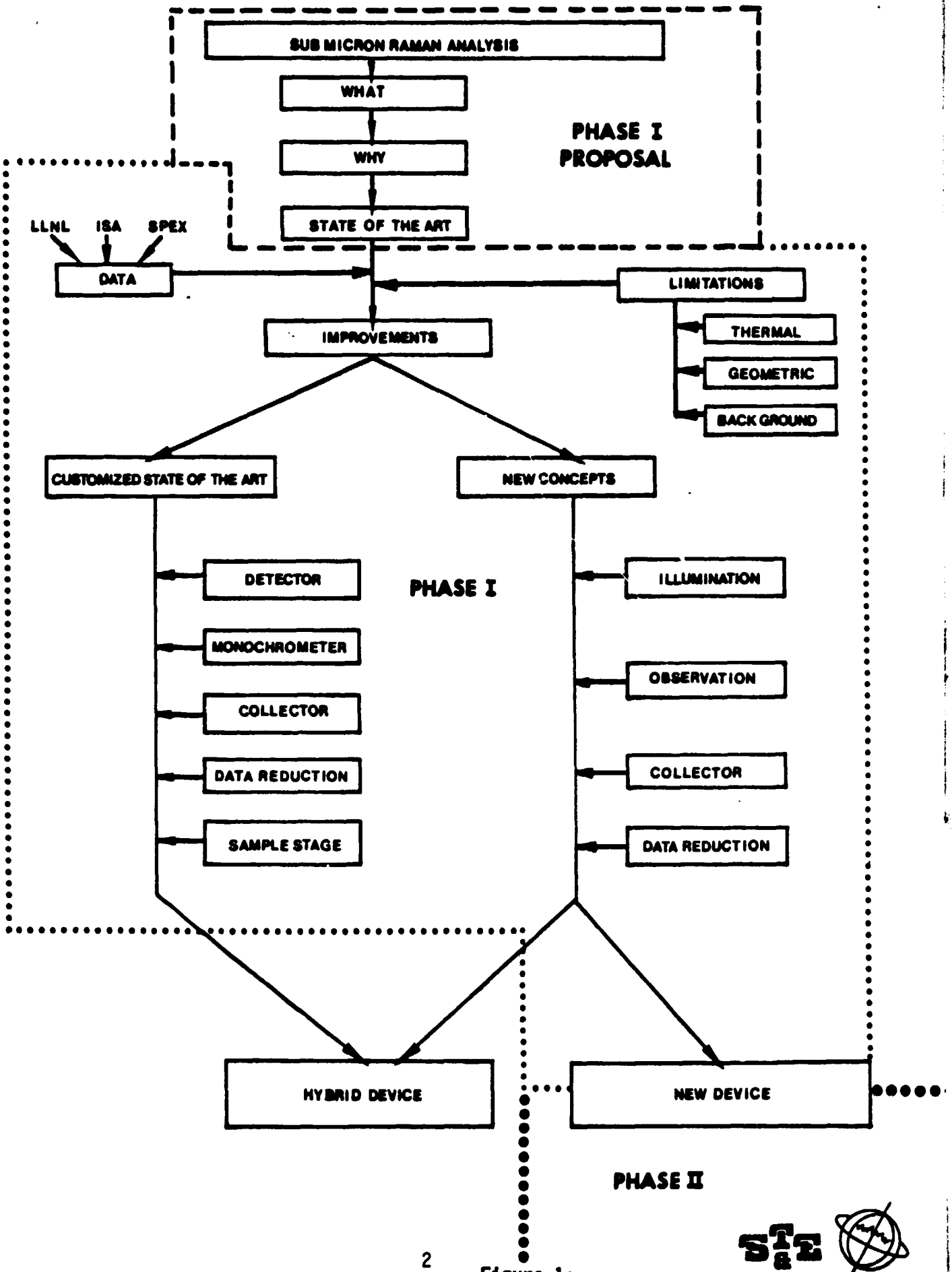

Figure 1:

early 1984 as a response to NASA SBIR solicitation 84-1, research area 08-12. The initial response was technical proposal No. 08-12 7847. The proposal itself represented considerable research into the nature of the NASA problem area, the identification of a solution and the establishment of a Phase I work plan. As a stand alone document, the Phase I proposal identified micro-Raman spectroscopy as the method to warrant further investigation for the analysis of micron and submicron aerosols of significant interest to NASA. Yet to be established at that time, in the field of micro-Raman, was the possibility of routine analyses of particles in the 0.1-1.0 micron (diameter) size. The proposal, therefore, responded to the need for such analysis, and directed the Phase I research to a fundamental evaluation of the state-of-the-art of micro-Raman spectroscopy. This evaluation was two-fold: (i) to assess, by comparison spectroscopy, the extant micro-Raman spectrometers, and (ii) to calculate, from first principles, the characteristics of a device that could routinely perform micro-Raman spectroscopy on particles as small as 0.1 micron.

The results of the spectroscopy evaluation are presented in Section 4.2. Here, representative samples were run on key micro-Raman spectrometers. The samples were selected by their applicability to determining ultimate sensitivity of the equipment and by their relevance to the NASA problem area.

The feasibility calculation is presented in Section 5.1. Here, a 0.3 micron diameter particle of representative physical characteristics (density, Raman cross-section and absorption coefficient) is analyzed as a potential micro-Raman target.

The results of the experimental and theoretical efforts generated the conclusions (Section 2.0) and recommendations (Section 3.0).

The choices in project direction (Phase II) were to either go with the current state-of-the-art (or a slightly customized version) of the LLNL

(Lawrence Livermore National Laboratory) spectrometer or to build a new-generation micro-Raman system. Based on the considerations and NASA's ultimate needs, the Phase II proposal addresses, in detail, the requirement for, and characteristics of, a new-generation spectrometer. At this point in the evaluation, it has been established that with the "new" micro-Raman particles to 0.3 μm should be easily measured and 0.1 μm remains a realistic overall goal. The Phase II micro-Raman instrument will not only meet today's needs but which, because of its CPU base, can be upgraded relatively easily as new requirements evolve.

1.2 Value of this Research to NASA

This micro-Raman feasibility study has demonstrated that a methodology exists and instrumentation is within reach which are compatible with the analysis of upper atmospheric aerosols. Moreover, this approach also gives chemical and crystal structure information which can be used in understanding the chemical reactions which have taken place.

The micro-Raman technology as presently understood, represents a major advancement in micro analysis. It is the only method for obtaining molecular information in the micro domain. The new-generation automated spectrometer will be suitable for both research and applied uses. It should become the key analytical device for studying gas/solid, liquid/solid, and solid/solid reactions. This leads to inclusion of micro-Raman in a large number of NASA's materials studies such as corrosion, oxidation, and erosion.

Applied/commercial uses for micro-Raman include the areas of catalysis, cell chemistry, medical research, process and quality control and air pollution. A specific industrial use would be in identifying impurities in semiconductors, nuclear detectors, and ultrapure materials.

2.0 Conclusions

The feasibility of identifying and quantifying micron and submicron collected atmospheric aerosols using micro-Raman techniques has been demonstrated during this Phase I task. During this effort micro-Raman spectra have been taken of particles of potential interest to NASA, existing "so-called" micro-Raman systems have been evaluated, a new-generation micro-Raman spectrometer has undergone preliminary design and performance calculations have been made for the new instrument. Based on these considerations, the following specific conclusions have been drawn:

(a) Commercial micro-Raman spectrometers give adequate Raman spectra for aerosols $\approx$ 2 μm.

(b) The micro-Raman spectrometer at LLNL (Lawrence Livermore National Laboratory) gives good Raman spectra for particles $\approx$1 μm.

(c) Definitive Raman spectra can be obtained using the LLNL instrument for $\approx$1 μm aerosols whose compositions are of interest to NASA.

(d) Inherent problems in micro-Raman spectroscopy include: (i) sample fluorescence (cannot be eliminated), (ii) substrate fluorescence (can be avoided if laser spot is smaller than sample), (iii) elastic scattering (characteristic of sample), and (iv) detector noise (can be minimized by careful selection).

(e) Problems which are the bain of all existing systems and which are solved by the new instrument design are: (i) size of the laser spot at the sample (much too large), (ii) sample viewing, (iii) sample screening, (iv) sample positioning, (v) spectrometer set-up and alignment, (vi) long-term frequency and intensity calibration, (vii) the use of a single optical system for both excitation and viewing (increases background, causes operational difficulties, represents a potential eye hazard) and (viii) need for a sophisticated operator.

(f) It is possible to design and build (using proven components) an automated user-friendly micro-Raman spectrometer capable of analyzing aerosols at least as small as 0.3 μm.

3.0 Recommendations

The research during Phase I has substantiated the potential of micro-Raman as a practical, routine method for identifying and quantifying collected aerosol samples. The recommendations listed below fall into two areas: (i) the construction of a next-generation micro-Raman spectrometer (to be proposed for Phase II) and (ii) measurements which should be made with the Phase II instrument. These include:

(a) Design, construct and test a completely automated next-generation micro-Raman spectrometer which has, as a minimum the following features: (i) a small (<0.3 μm) laser spot for sample illumination, (ii) sample viewing, (iii) sample preselection, (iv) ability to locate and place discrete particles, (v) easy set-up and alignment, (vi) internal frequency and intensity calibration, (vii) computer-controlled housekeeping and data gathering and processing capability, and (viii) user-friendly operation. This is covered in the Phase II proposal.

(b) Using the new micro-Raman spectrometer generate a library of micro-Raman spectra for aerosol compounds of interest to NASA. Initial work should be done on both 0.3 μm and 1.0 μm particles. If no difference in spectral characteristics are observed between the 0.3 μm and the 1.0 μm particles (after sufficient sampling), then 1.0 μm aerosols can be used exclusively. If the submicron particles yield spectra which are different from the larger ones (due to the fact that particle size is smaller than the wavelength of the irradiating light), then it will be necessary to continue with both sizes. This information can be stored in memory and used for spectral correlation, if desired.

(c) Prepare quantitative standards for the key aerosols and develop "look-up" curves for intensity vs concentration using the "new" spectrometer. This data can be stored in memory and used for comparison with the NASA unknown

particles.

(d) Analyze aerosols collected for NASA using the new micro-Raman spectrometer and the newly generated library (b) and "look-up" tables (c).

(e) Use the information gleaned in (b), (c) and (d) to determine the accuracy and reproducibility of the new micro-Raman system and to evaluate ease of operation.

4.0 The Micro-Raman Spectra of Solids

Most Raman data reported in the literature are for gases, liquids and solutions. Here, essentially, the phenomenon is that of light scattering by isolated molecules. Molecular interaction is considered, if necessary, as a perturbation and not as a primary effect. This approach, however, is not applicable to the interpretation, understanding and analytical application of the Raman spectra of solids. In crystals, the atoms, or ions, are set at small distances from one another and their displacement from the equilibrium positions are correspondingly small. The intermolecular distances, therefore, cannot be treated as a weak perturbation since they are the very reason a crystal (solid) exists. In fact, crystals are characterized by a regular three-dimensional arrangement of atoms and show a specific symmetry. This symmetry determines the individual properties of the crystal.

Raman spectroscopy is primarily concerned with crystal lattice dynamics. The Raman selection rules, however, ultimately depend on molecular and crystal symmetries and this information can be of great help in elucidating crystal structure. This may be important in the measurement of atmospheric aerosols as it can provide historical information about the particle.

4.1 Micro-Raman Spectroscopy

The Raman or micro-Raman Effect is a scattering phenomenon similar to other light-scattering processes, such as Rayleigh and Brillouin scattering. In Raman scattering, the incident radiation is scattered at a shifted frequency. This shift in frequency results from the effects of rotational and vibrational motion on the electronic polarizability of the molecules which scatter the light. The observed Raman shifts correspond to energy differences between different rotational and vibrational states of the molecules. Each type of molecule has its own characteristic set of rotational and vibrational energy level differences, so that Raman scattering spectroscopy provides a reliable

technique for "fingerprinting" different molecules.

Different molecules are characterized by specific Raman shifts and by specific Raman scattering cross-sections. The magnitude of the Raman shifts provide unambiguous identifications for different types of molecules. Raman cross-sections are measures of the amount of Raman scattered radiation produced when a molecule is irradiated. The total scattering cross-section is an area, typically on the order of 10^{-29} cm^2 for solids, which provides a quantitative measure of the amount of Raman scattering produced by a single molecule. It is defined such that the total power which is Raman scattered by a molecule (photons/s) is equal to the product of the total Raman cross-section and the irradiance of the incident radiation (photons/cm^2 s). Raman cross-sections are generally inversely proportional to the fourth power of the incident wavelength. The amount of Raman scattering per steradian in a particular direction (relative to that of the incident radiation) is measured by the differential scattering cross-section (cm^2/steradian). The angular distribution of scattered light is a function of the incident polarization as well as angle. This information is essential for solid state Raman spectroscopy and the next-generation micro-Raman spectrometer is designed to preserve this information.

4.2 Information Available From Micro-Raman Data

In the present application the emphasis is on the identification and quantification of micron and submicron aerosols. Here the position of the micro-Raman spectral lines on the frequency ramp can be used to "fingerprint" a molecule. The paucity of lines (as compared to infrared techniques) and their narrow width (as compared to fluorescence measurements) makes unambiguous identification possible, even in mixtures. In fact, the micro-Raman lines in solids are sufficiently narrow and strong so that the main constituents in a submicron particle can be identified.

An example of the ability of micro-Raman to distinguish between compounds can be shown using the sulfates. Here the micro-Raman shifts for SO_4^{-2} are as follows: $(NH_4)_2SO_4$ = 974 cm^{-1}, K_2SO_4 = 981 cm^{-1}, Na_2SO_4 = 995 cm^{-1}, and Li_2SO_4 = 1003 cm^{-1}. From this data it can be seen that the cation which is associated with the SO_4^{-2} affects the shift and thus the sulfate compound is identifiable. It should also be noted that the smaller the cation, the greater the shift. It is of course also possible to identify mixed ammonium compounds by the micro-Raman shift of the anion, i.e. NH_4NO_3 = 709 and 1043 cm^{-1}, $(NH_4)_3PO_4$ = 924 cm^{-1}, and a previously mentioned, $(NH_4)_2SO_4$ = 974 cm^{-1}.

A second example, which demonstrates the power of micro-Raman for species identification is presented by Ishida and Ishitani [1] who looked at the thin films on the surfaces of silver electrical contacts. Auger electron spectroscopy (AES), the most used method of surface analysis, could only identify the presence of Ag, S, C, and O but the micro-Raman recognized Ag_2SO_4, $AgHS_2O_7$ and free carbon thus giving incite into the mechanisms of the thin film formation.

Quantitative information is available from micro-Raman in either of two ways. In each case the initial step is to obtain reference spectra as a function of concentration for the compound of interest. The most common approach to quantification is to select a strong line and determine how its intensity changes with concentration and develop a "look up" table to which all unknowns can be compared. This will give reasonable results but could have errors due to a variety of unaccounted for parameters such as temperature, crystal defects, conditions under which the aerosol formed, etc. A better approach, therefore, is to look for situations, if they exist, where the ratio of two lines is concentration dependent. This essentially eliminates all extraneous unknowns and improves the reliability of the analysis. For example, in solution $(NH_4)_2SO_4$ concentrations can be accurately obtained by ratioing the 981 cm^{-1} and 1100 cm^{-1} line intensities [2]. In a like manner it may be

possible to ratio the 974 cm^{-1} and 1100 cm^{-1} line intensities in crystalline $(NH_4)_2SO_4$.

Although qualitative and quantitative analysis of small particles is the objective of this work, advantage should be taken of the wealth of structural information available from the micro-Raman data. In particular a great deal of background may be generated about the conditions and mechanisms of the particle formation. In order to extract the necessary data, however, requires that the micro-Raman system retain all polarization information and this should be a criterion for the next-generation micro-Raman system.

One example of the use of micro-Raman would be to tell the difference between naturally occurring materials and synthesized ones. This permits one to determine if a reaction has taken place. For example, Fraas [3] et al have shown that Raman can be used to tell the difference between synthetic and natural $MgAl_2O_4$ crystals.

4.3 Micro-Raman Spectra

As stated previously, the intent of the Phase I research was to demonstrate the potential of micro-Raman to identify and quantify the species in micrometer and submicrometer particles. In doing this feasibility study all existing "so-called" micro-Raman spectrometers were evaluated. These included the two commercial units built by Spex and ISA (Instrument SA) and the "one-of-a-kind" system at LLNL (Lawrence Livermore National Laboratory). The objective of this exercise was to determine: (i) what is the smallest aerosol that can be analyzed by extant spectrometers. (ii) what types of particles, of interest to NASA, are amenable to micro-Raman analysis. (iii) what measurement times are required and are they compatible with avoiding sample destruction by either photo or thermal decomposition.

There can be no specific limits that can be established to answer these

questions and the best approach is to present spectral data for evaluation. Figures 2 through 24 represent typical micro-Raman spectra taken on the three instruments. It should be noted that the SPEX instrument is really not suitable for aerosols approaching 1 μm and only one acceptable spectrum is presented. Carbon was used as a standard of reference. Figure 2 is highly oriented carbon run on the ISA instrument. The spectral peak at 1580 cm^{-1} is representative of this material [4]. 25 mW of laser power at 514.5 nm and 2,250 seconds (37.5 minutes) was required to measure a 3 μm particle. This is not acceptable because these operational conditions essentially prohibit the analysis of any aerosol with even moderate thermal or photo sensitivity. Figure 3 is the same size carbon particle run on the LLNL machine. Here laser power is 1 mW and analysis time is 300 s (5 minutes). The small peak at 1360 cm^{-1} indicates that the sample lattice has some disorder. Figure 4 is a repeat of Figure 3 with the laser power raised to 2.5 mW. Here excellent signal to noise is noted with both the 1580 cm^{-1} and 1360 cm^{-1} lines fully resolved. Less than 5 mW of laser power at 514.5 nm and analysis times of 300 s or less should permit most aerosols 1 micrometer or larger to be analyzed. No carbon data was obtained with the SPEX system. Figures 5 and 6 are spectra of carbon fibers run on the ISA instrument. Important to note for these spectra is the 40 mW and 50 mW of laser power and the long analysis times.

Figures 7 and 8 are the spectra for carbon with a highly disordered lattice. Figure 7 was obtained using the ISA spectrometer. In order to obtain this spectrum not only were high laser powers and long observation times used, but the baseline had to be artificially raised above zero to help overcome the background. The peaks at 1360 cm^{-1} and 1620 cm^{-1} are indicative of disordered carbon. It is, however, difficult to see that the 1580 cm^{-1} line is missing. In Figure 8, run on the LLNL instrument, laser power is only 1.4 mW and analysis time is only 300 s. The baseline is at zero and the 1360 cm^{-1} and 1620 cm^{-1}

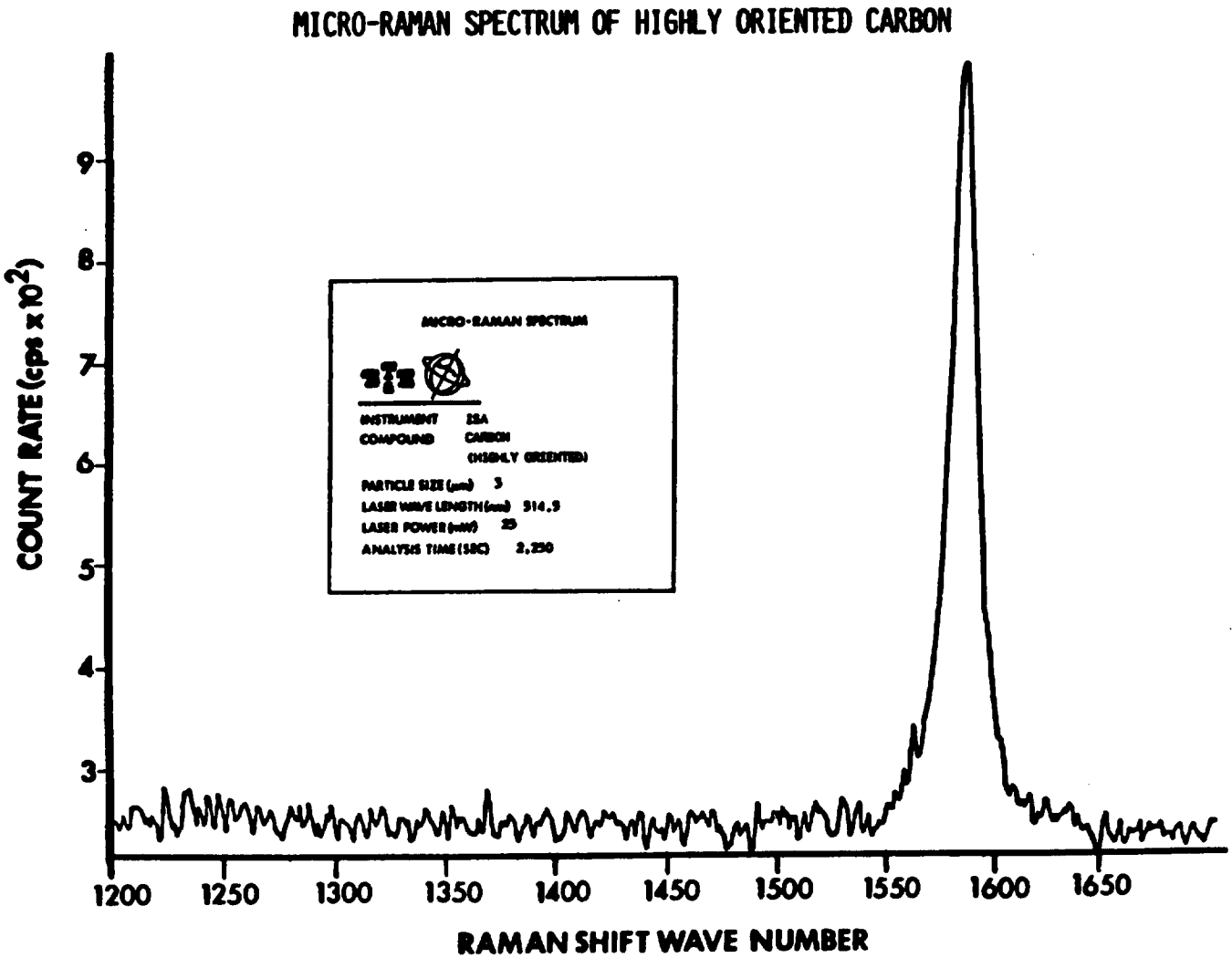
MICRO-RAMAN SPECTRUM OF HIGHLY ORIENTED CARBON
COUNT RATE (cps x 10²)
9
8
7
6
5
4
3
MICRO-RAMAN SPECTRUM
INSTRUMENT ISA
COMPOUND CARBON
(HIGHLY ORIENTED)
PARTICLE SIZE (μm) 3
LASER WAVE LENGTH (nm) 514.5
LASER POWER (mW) 25
ANALYSIS TIME (SEC) 2,250
1200
1250
1300
1350
1400
1450
1500
1550
1600
1650
RAMAN SHIFT WAVE NUMBER

Figure 2:

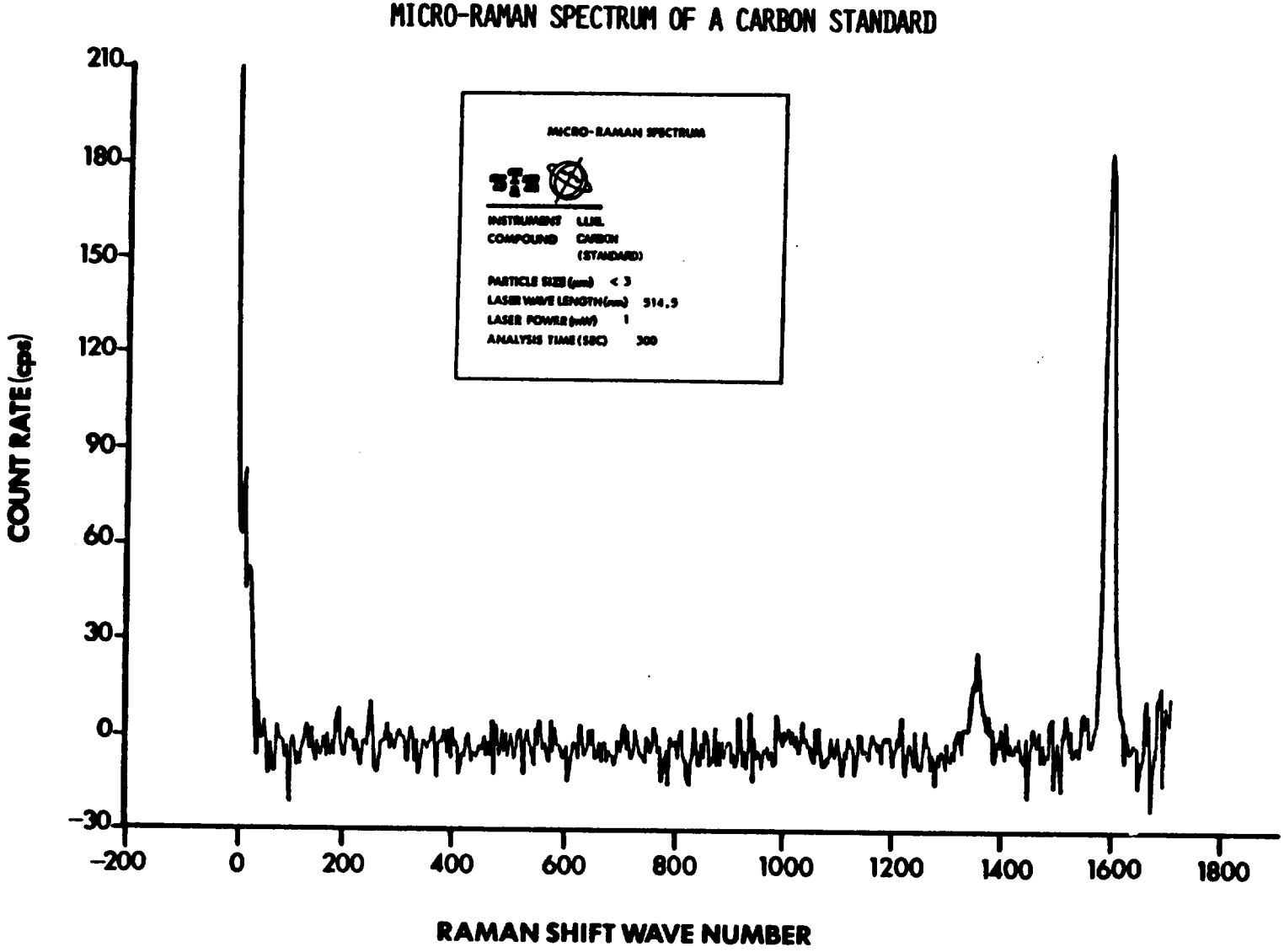
MICRO-RAMAN SPECTRUM OF A CARBON STANDARD
MICRO-RAMAN SPECTRUM
INSTRUMENT LLBL
COMPOUND CARBON
(STANDARD)
PARTICLE SIZE (μm) < 3
LASER WAVE LENGTH (nm) 514.5
LASER POWER (mW) 1
ANALYSIS TIME (SEC) 300
COUNT RATE (cps)
210
180
150
120
90
60
30
0
-30
-200
0
200
400
600
800
1000
1200
1400
1600
1800
RAMAN SHIFT WAVE NUMBER

Figure 3:

MICRO-RAMAN SPECTRUM OF A CARBON STANDARD

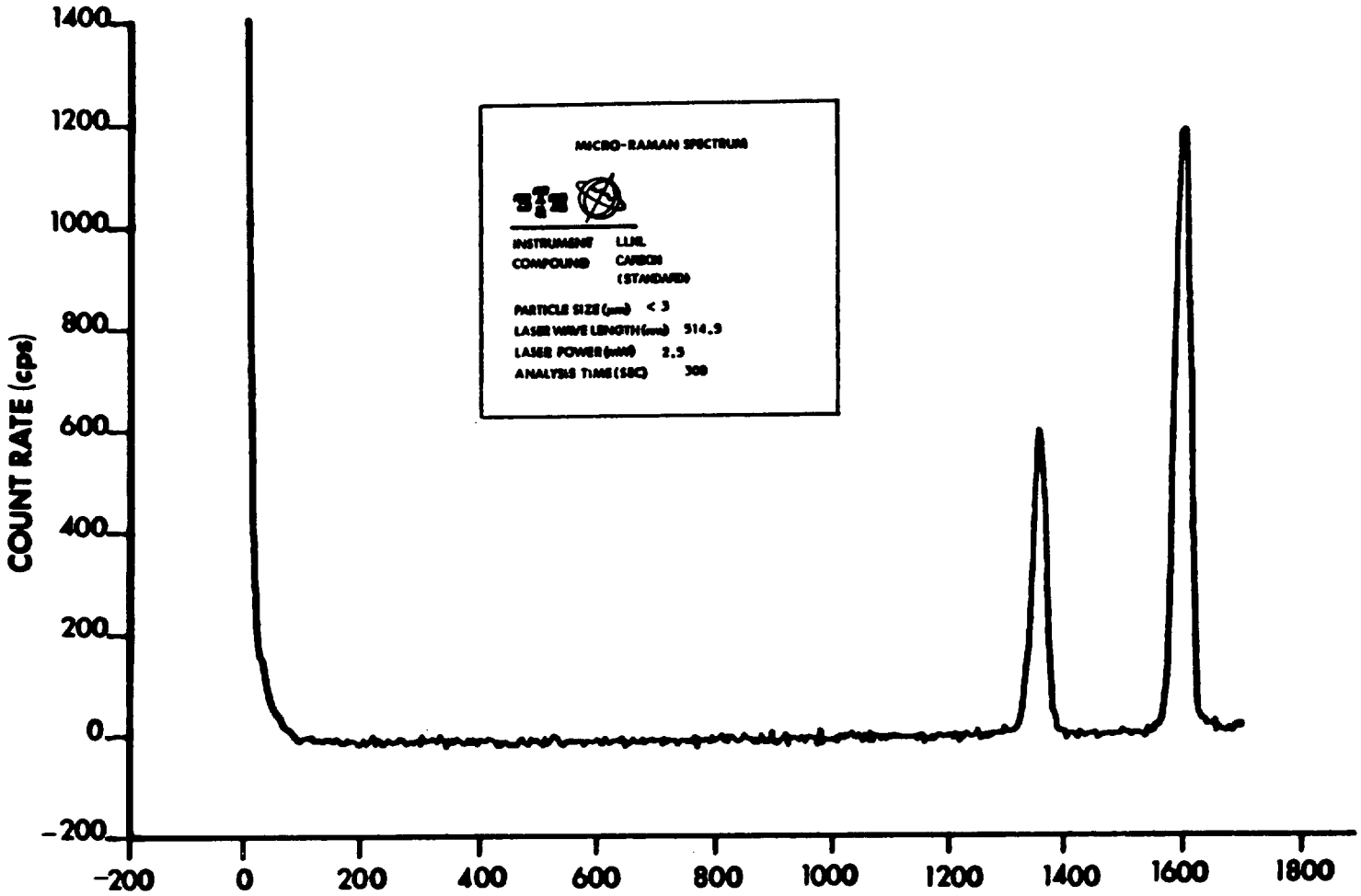

Figure 4:

MICRO-RAMAN SPECTRUM OF CARBON FIBER FROM POLYACRYLONITRILE

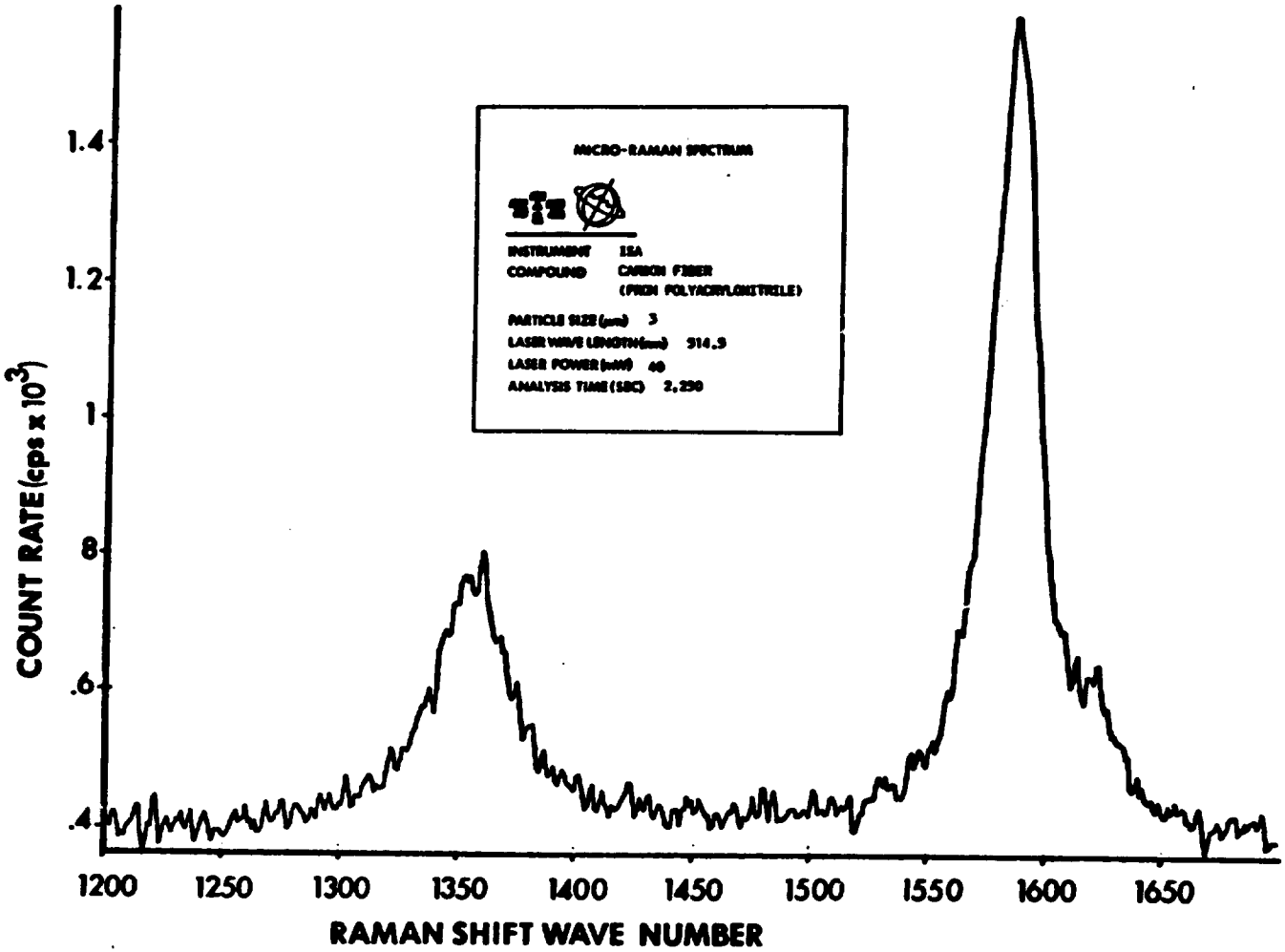

Figure 5:

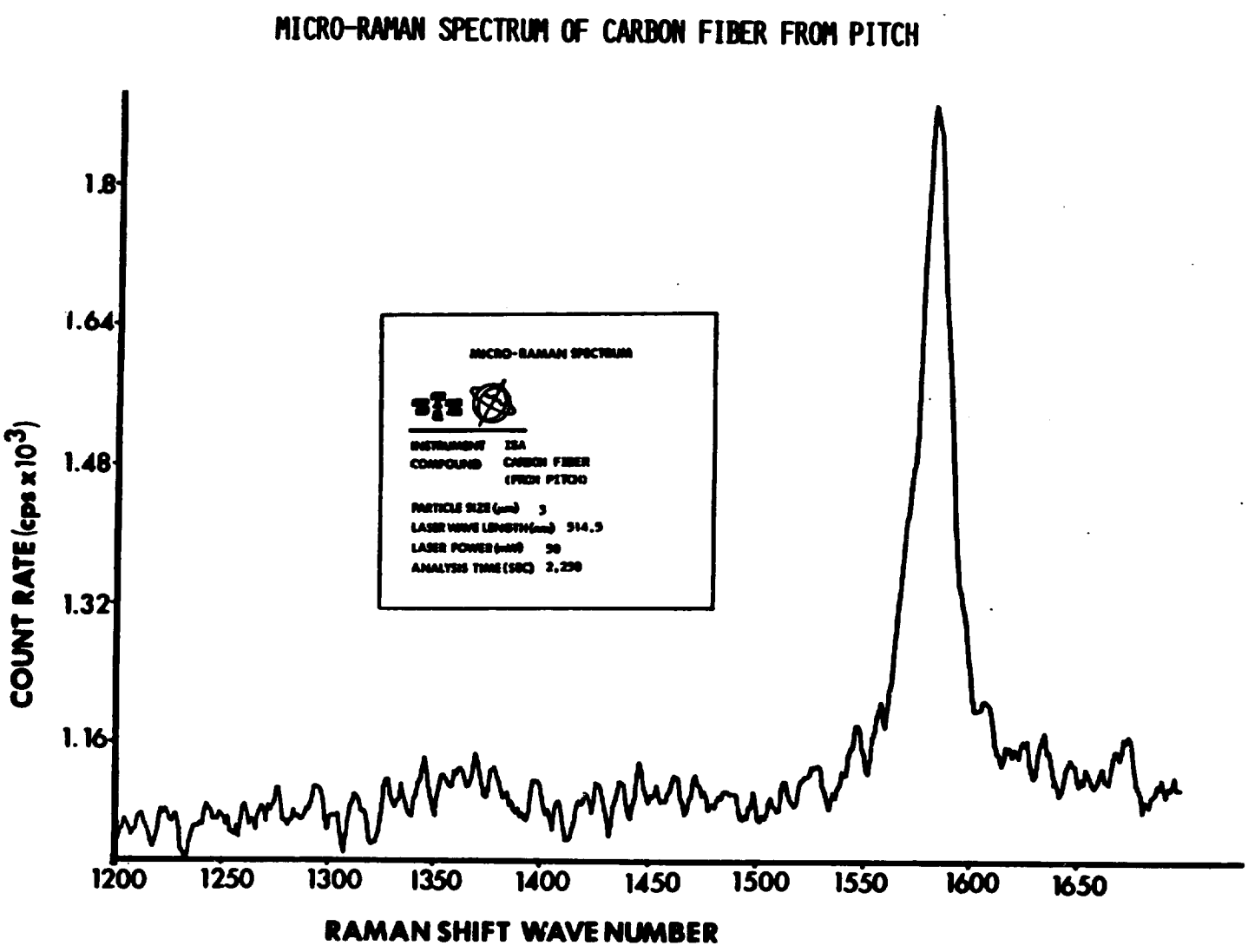
MICRO-RAMAN SPECTRUM OF CARBON FIBER FROM PITCH
MICRO-RAMAN SPECTRUM
INSTRUMENT ISA
COMPOUND CARBON FIBER
(FROM PITCH)
PARTICLE SIZE (μm) 3
LASER WAVE LENGTH (nm) 514.5
LASER POWER (mW) 30
ANALYSIS TIME (SEC) 2,250
COUNT RATE (cps x 10^3)
1.8
1.64
1.48
1.32
1.16
1200
1250
1300
1350
1400
1450
1500
1550
1600
1650
RAMAN SHIFT WAVE NUMBER

Figure 6:

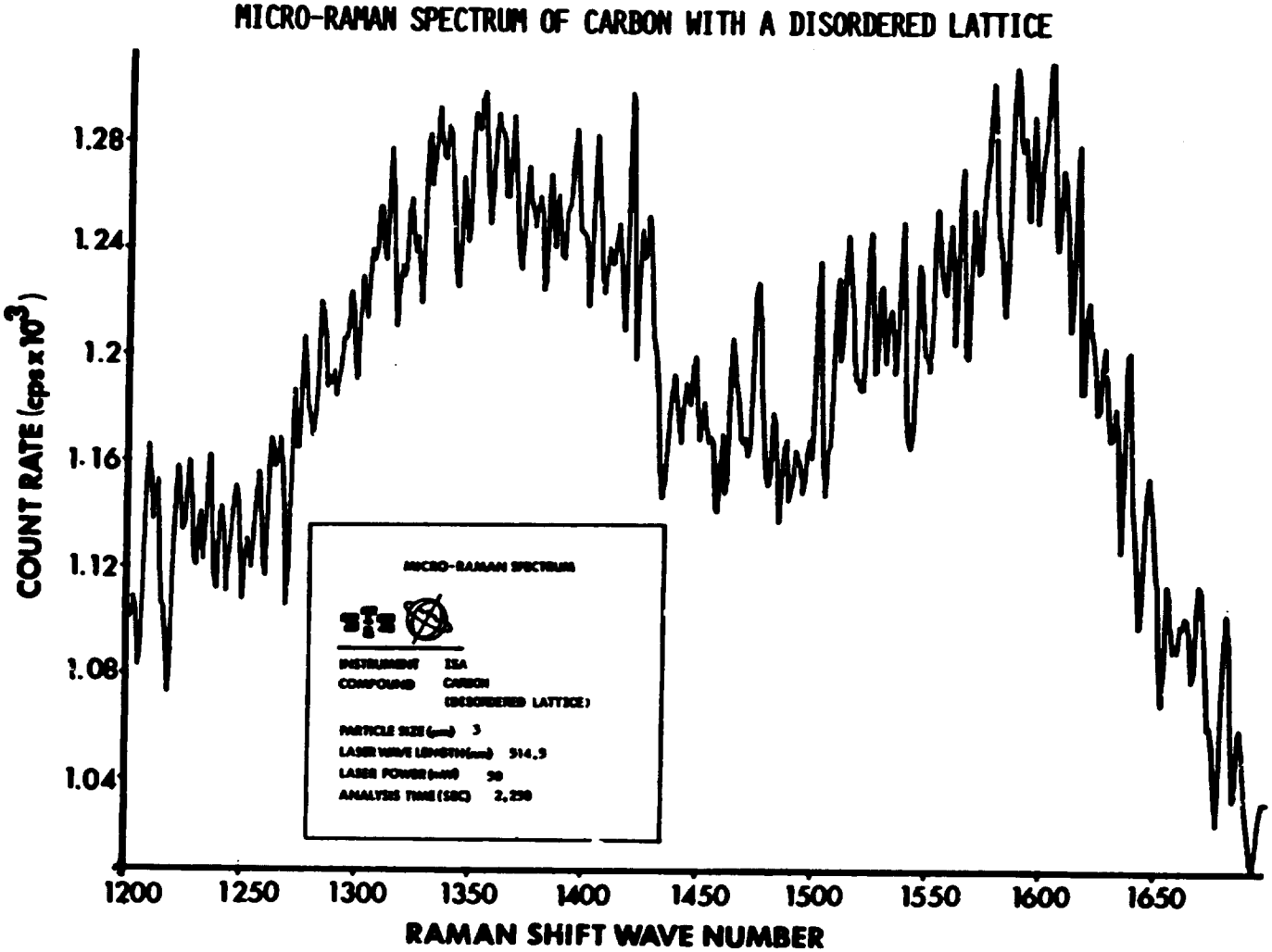
MICRO-RAMAN SPECTRUM OF CARBON WITH A DISORDERED LATTICE
COUNT RATE (cps x 10³)
1.28
1.24
1.2
1.16
1.12
1.08
1.04
1200
1250
1300
1350
1400
1450
1500
1550
1600
1650
RAMAN SHIFT WAVE NUMBER
MICRO-RAMAN SPECTRUM
INSTRUMENT ISA
COMPOUND CARBON
(DISORDERED LATTICE)
PARTICLE SIZE (μm) 3
LASER WAVE LENGTH (nm) 514.5
LASER POWER (mW) 50
ANALYSIS TIME (SEC) 2,250

Figure 7:

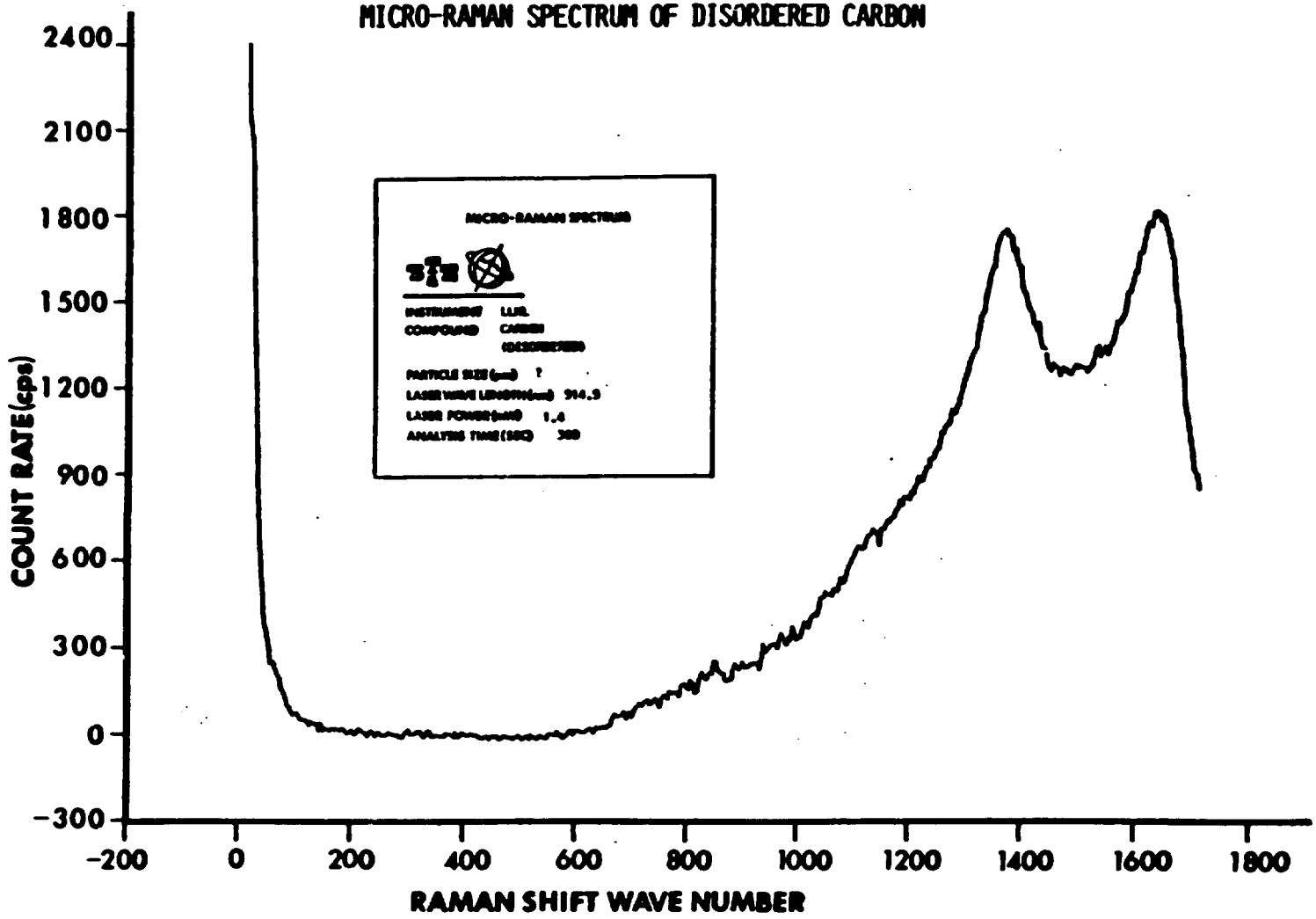
MICRO-RAMAN SPECTRUM OF DISORDERED CARBON
COUNT RATE(cps)
2400
2100
1800
1500
1200
900
600
300
0
-300
-200
0
200
400
600
800
1000
1200
1400
1600
1800
RAMAN SHIFT WAVE NUMBER

Figure 8:

lines are present with acceptable signal to noise. Furthermore, the 1580 cm^{-1} peak is obviously missing indicating a completely disordered carbon lattice. From the carbon data it is obvious that any carbon particles collected in the atmosphere will be identifiable.

The presence of sulfate in the atmosphere is expected as $(NH_4)_2SO_4$. Figure 9 is the micro-Raman spectrum of $(NH_4)_2SO_4$ taken on the LLNL system. Here the particle size is 1 μm, laser power is 1.4 mW at 514.5 nm and the analysis time is 300 s. The strong line at 974 cm^{-1} is indicative of crystalline $(NH_4)_2SO_4$. It is important to note that the information available for liquid aerosols [5] of $(NH_4)_2SO_4$, NH_4HSO_4 and H_2SO_4 are not applicable to a solid state system. From the work of Rosen and Novakov [6] if NH_4HSO_4 were present its spectrum will contain a single line at 876 cm^{-1} and a doublet between 1010 and 1045 cm^{-1}. H_2SO_4 (not likely) would appear at about 907 cm^{-1}, 1045 cm^{-1} and 1179 cm^{-1}. Neither NH_4HSO_4 nor H_2SO_4 have been observed during this work. Figure 10 is a repeat of Figure 9 using an expanded scale to enhance the presence of the smaller peaks. Here it can be seen that by using proper scale expansions, the concentration of $(NH_4)_2SO_4$ in a mixture, can probably be obtained by ratioing the 974 cm^{-1} and 1090 cm^{-1} line intensities. Figure 11 is the expanded $(NH_4)_2SO_4$ spectrum obtained using only 0.7 mW of laser power. Here it can be seen that reducing the power has decreased the background (fluorescence) without greatly reducing spectral quality.

Figures 12, 13, and 14 are spectra taken for CeO_2. This compound was chosen to demonstrate the ultimate capability of the extant LLNL unit. The three spectra have been chosen to demonstrate the minimum particle size, analysis time and laser power. Figure 12 is the spectrum of a 12 μm particle using 5 mW of 514.5 nm laser power and an analysis time of 60 s. Not only is the 463 cm^{-1} line reported in the literature [7] shown, but additional detail is

MICRO-RAMAN SPECTRUM OF AMMONIUM SULFATE

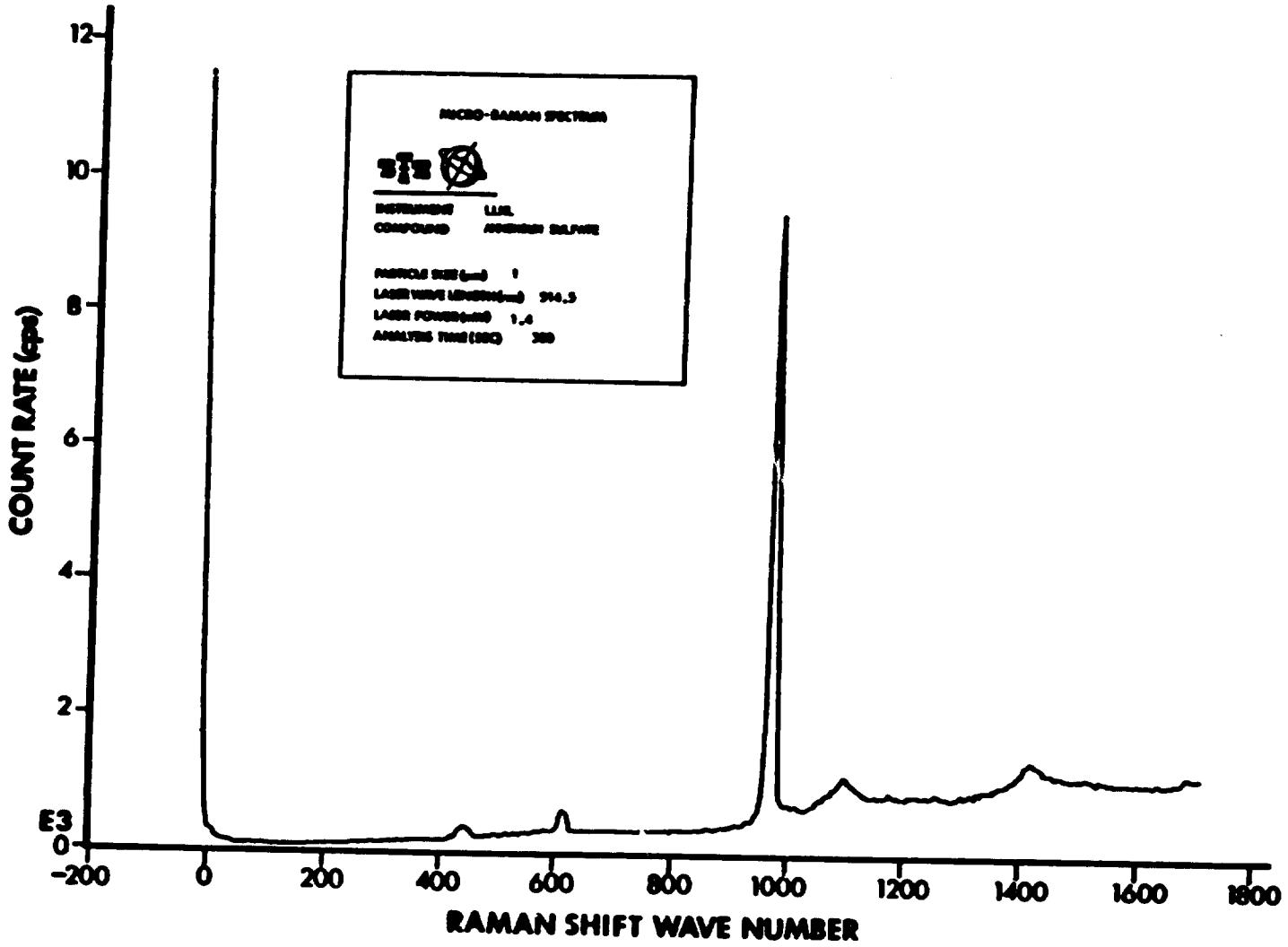

Figure 9:

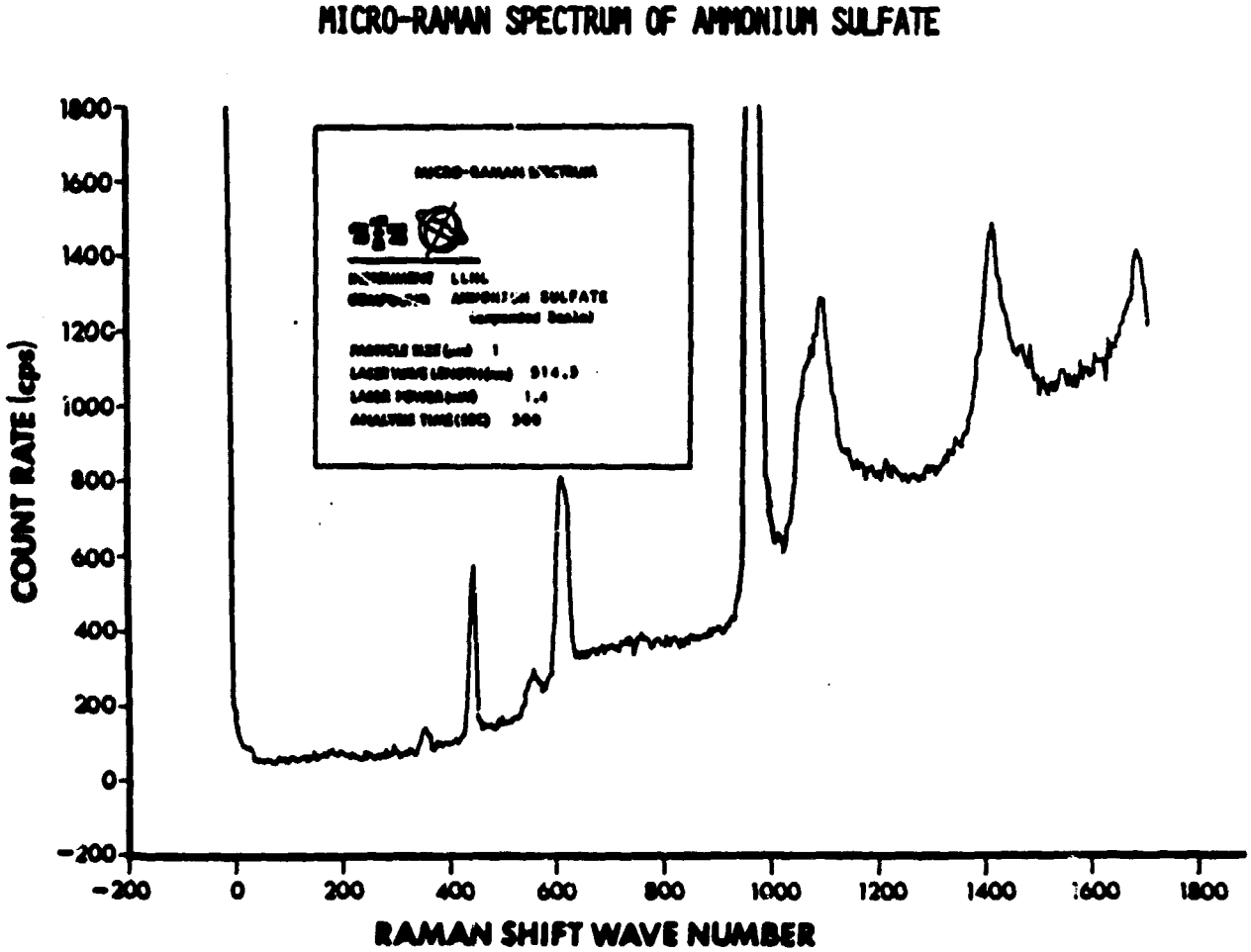
MICRO-RAMAN SPECTRUM OF AMMONIUM SULFATE
COUNT RATE (cps)
1800
1600
1400
1200
1000
800
600
400
200
0
-200
-200
0
200
400
600
800
1000
1200
1400
1600
1800
RAMAN SHIFT WAVE NUMBER

Figure 10:

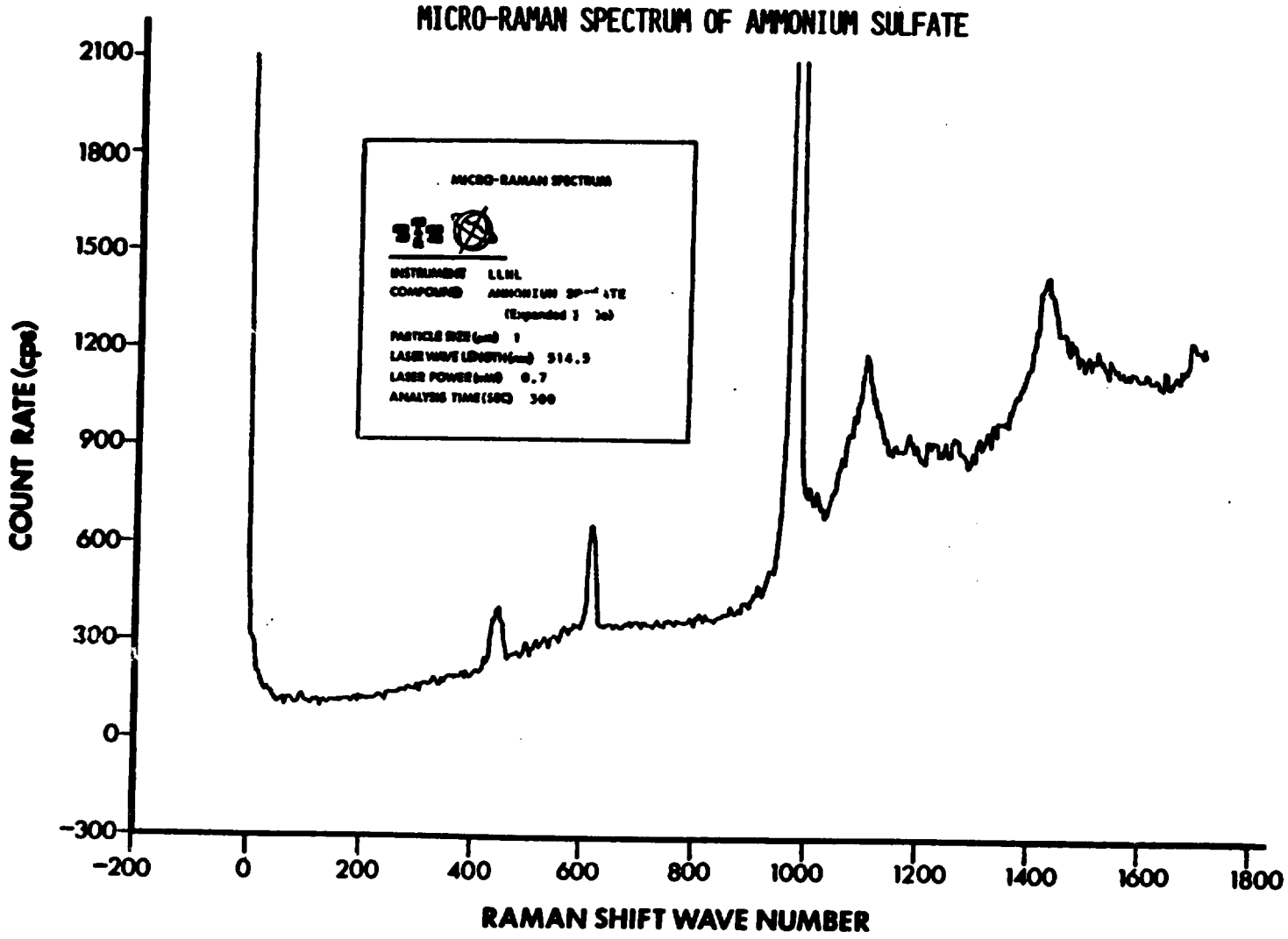
MICRO-RAMAN SPECTRUM OF AMMONIUM SULFATE
COUNT RATE (cps)
2100
1800
1500
1200
900
600
300
0
-300
-200
0
200
400
600
800
1000
1200
1400
1600
1800
RAMAN SHIFT WAVE NUMBER
MICRO-RAMAN SPECTRUM
INSTRUMENT LLNL
(Expanded 3)
LASER WAVE LENGTH(nm) 514.5
LASER POWER(mW) 0.7
ANALYSIS TIME(SEC) 300

Figure 11:

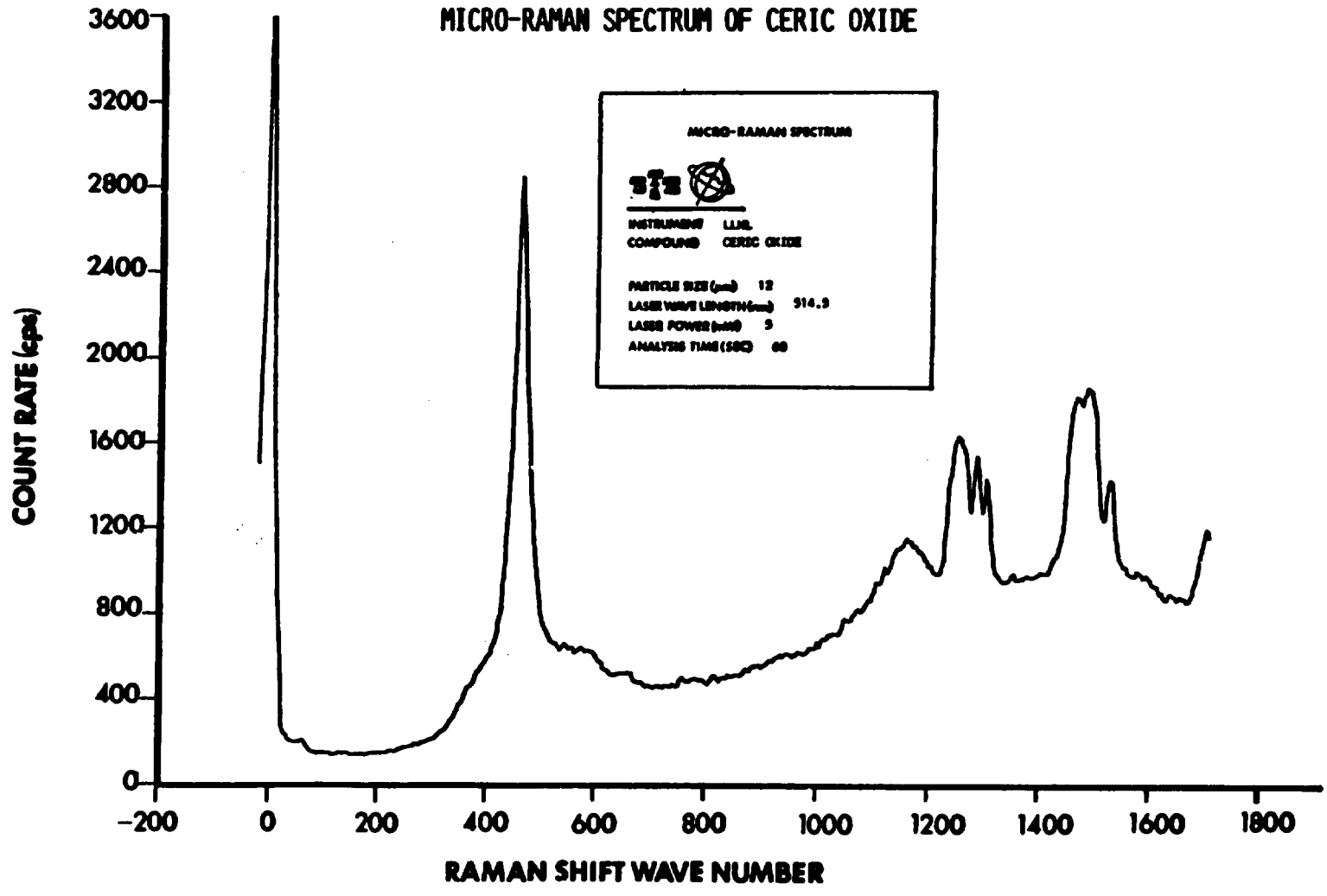
MICRO-RAMAN SPECTRUM OF CERIC OXIDE
MICRO-RAMAN SPECTRUM
INSTRUMENT LLNL
COMPOUND CERIC OXIDE
PARTICLE SIZE (μm) 12
LASER WAVE LENGTH (nm) 514.5
LASER POWER (mW) 5
ANALYSIS TIME (SEC) 60
COUNT RATE (cps)
3600
3200
2800
2400
2000
1600
1200
800
400
0
-200
0
200
400
600
800
1000
1200
1400
1600
1800
RAMAN SHIFT WAVE NUMBER

Figure 12:

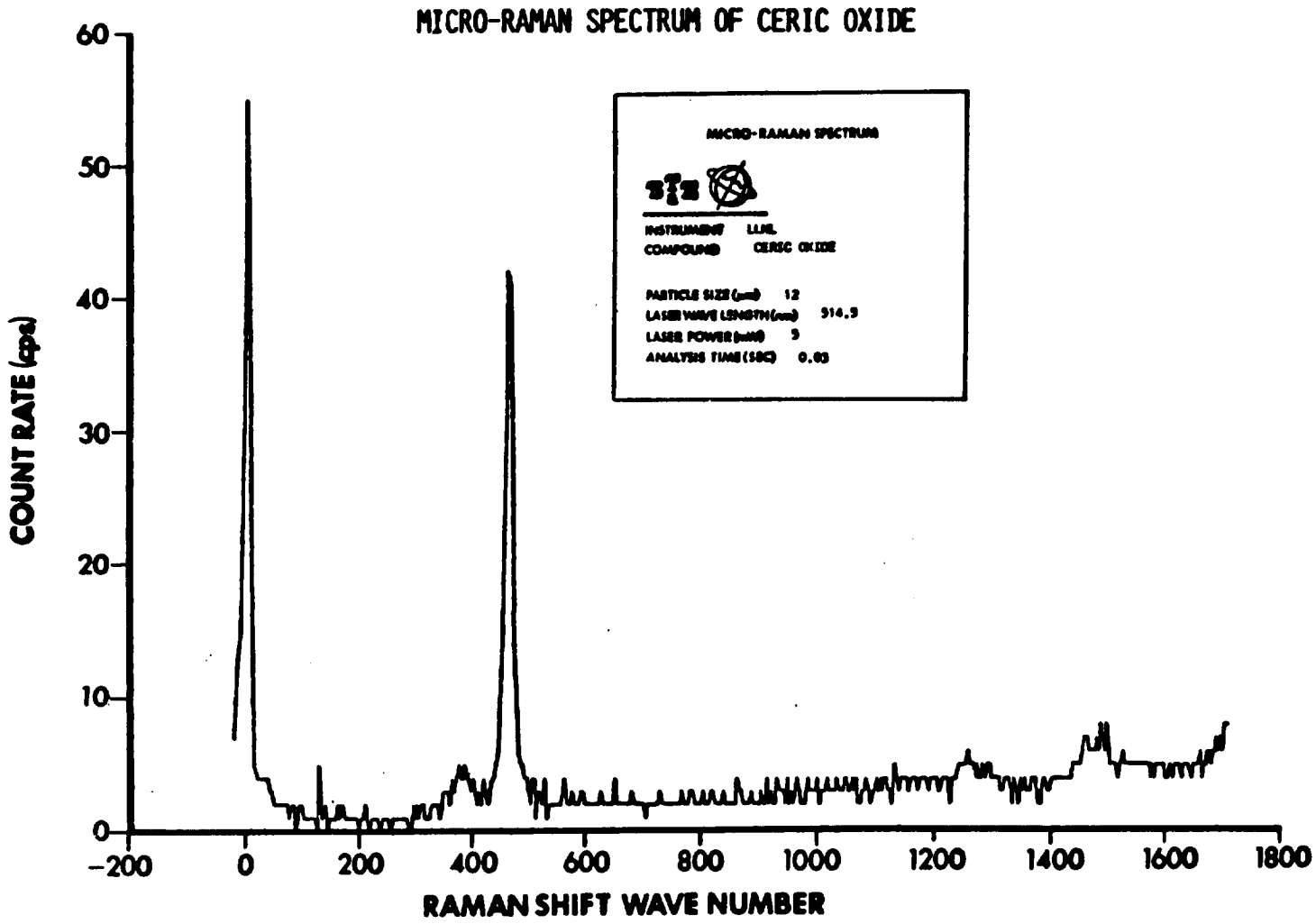
MICRO-RAMAN SPECTRUM OF CERIC OXIDE
MICRO-RAMAN SPECTRUM
INSTRUMENT LLNL
COMPOUND CERIC OXIDE
PARTICLE SIZE (μm) 12
LASER WAVE LENGTH (nm) 514.5
LASER POWER (mW) 5
ANALYSIS TIME (SEC) 0.03
COUNT RATE (cps)
60
50
40
30
20
10
0
-200
0
200
400
600
800
1000
1200
1400
1600
1800
RAMAN SHIFT WAVE NUMBER

Figure 13:

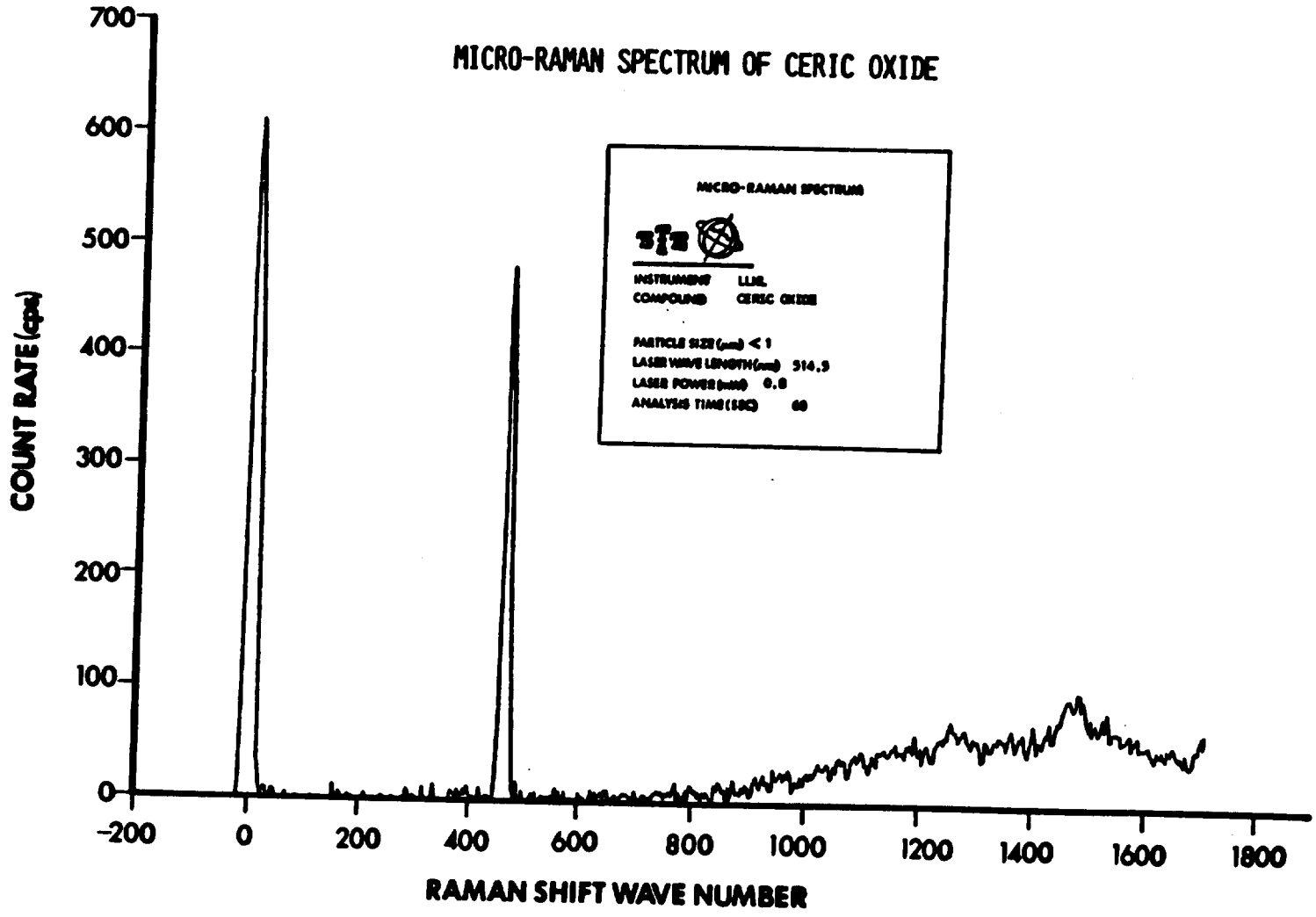
MICRO-RAMAN SPECTRUM OF CERIC OXIDE
MICRO-RAMAN SPECTRUM
INSTRUMENT LLNL
COMPOUND CERIC OXIDE
PARTICLE SIZE (μm) < 1
LASER WAVE LENGTH (nm) 514.5
LASER POWER (mW) 0.8
ANALYSIS TIME (SEC) 60
COUNT RATE (cps)
700
600
500
400
300
200
100
0
-200
0
200
400
600
800
1000
1200
1400
1600
1800
RAMAN SHIFT WAVE NUMBER

Figure 14:

evident between 1200 and 1320 cm^{-1} and 1400 and 1565 cm^{-1}. This later information is important in separating the oxides because many have almost the same identical primary peak, i.e., ThO_2 = 465 cm^{-1}, UO_2 = 467 cm^{-1}, HfO_2 = 495 cm^{-1} and ZrO_2 = 476 cm^{-1}. Figure 13 is the spectrum of the same particle as shown in Figure 12 except that the observation time has been reduced to 0.03 s! Although much of the spectral detail has been lost, the main peak is present with good signal to noise. Analyses using only 5 mW of laser power for only 0.03 s should make it possible to identify and quantify even the most photo- or thermally-sensitive aerosol. Figure 14 probably depicts the present state-of-the-art in micro-Raman spectroscopy - a 1 μm particle, 0.8 mW of laser power at 514.5 nm, 60 s analysis time, and a signal to noise of 70.

Figure 15 is included because it demonstrates the ability of micro-Raman to analyze thermally-sensitive compounds such as naphthaline (volatilizes appreciably at room temperature, bp_{760} 218°C) without loss or damage of the particle. Figure 15a is for a 5 μm naphthalene particle whose spectrum was obtained in 12 s using 2 mW of 514.5 nm laser power. Figure 15b is for a 70 μm aerosol run under the same conditions. Comparison of the spectra in Figure 15a to 15b shows that the spectra are identical, except for signal to noise, thus indicating that the smaller particle remained intact during analysis. In addition, the micro-Raman spectral data can be matched to standard Raman spectra for naphthalene [8].

Wilkinson [9] has assembled the data on Al_2O_3, Cr_2O_3 and Fe_2O_3. The results of their compilation are shown in Table 4.1. This information on Fe_2O_3 can be compared directly to the micro-Raman spectrum for α-Fe_2O_3 in Figure 16. The ISA spectrometer required 70 mW of 514.5 nm laser power for 1,500 s to measure a 3 μm particle. On the other hand, with the exception of the 245 a 500 cm^{-1} peaks, which are hard to identify (but can be extracted), all of the shifts listed in the Table are evident in the spectral data. In Figure 17 the

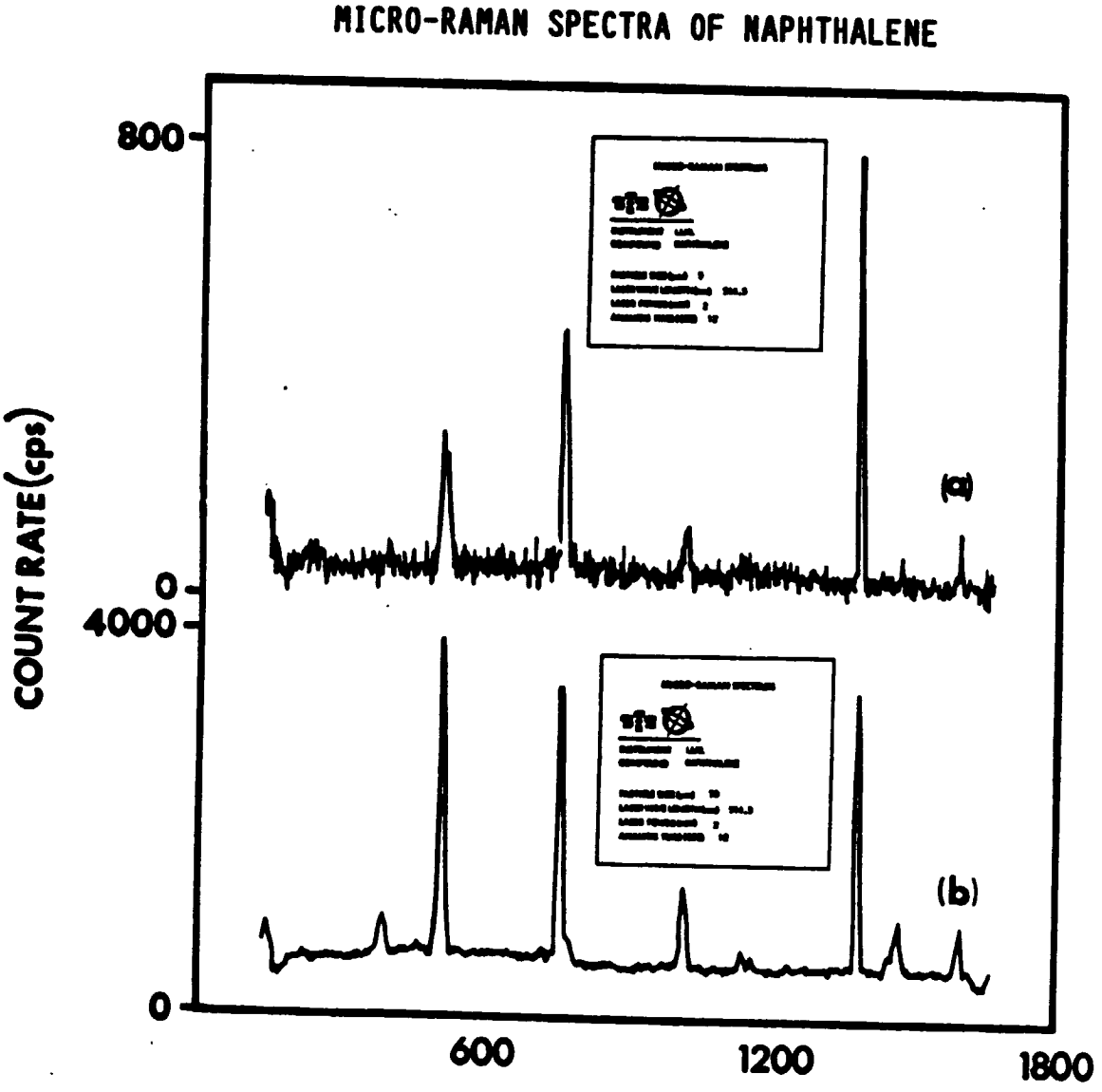
MICRO-RAMAN SPECTRA OF NAPHTHALENE
COUNT RATE(cps)
800
0
4000
0
600
1200
1800
(a)
(b)

Figure 15:

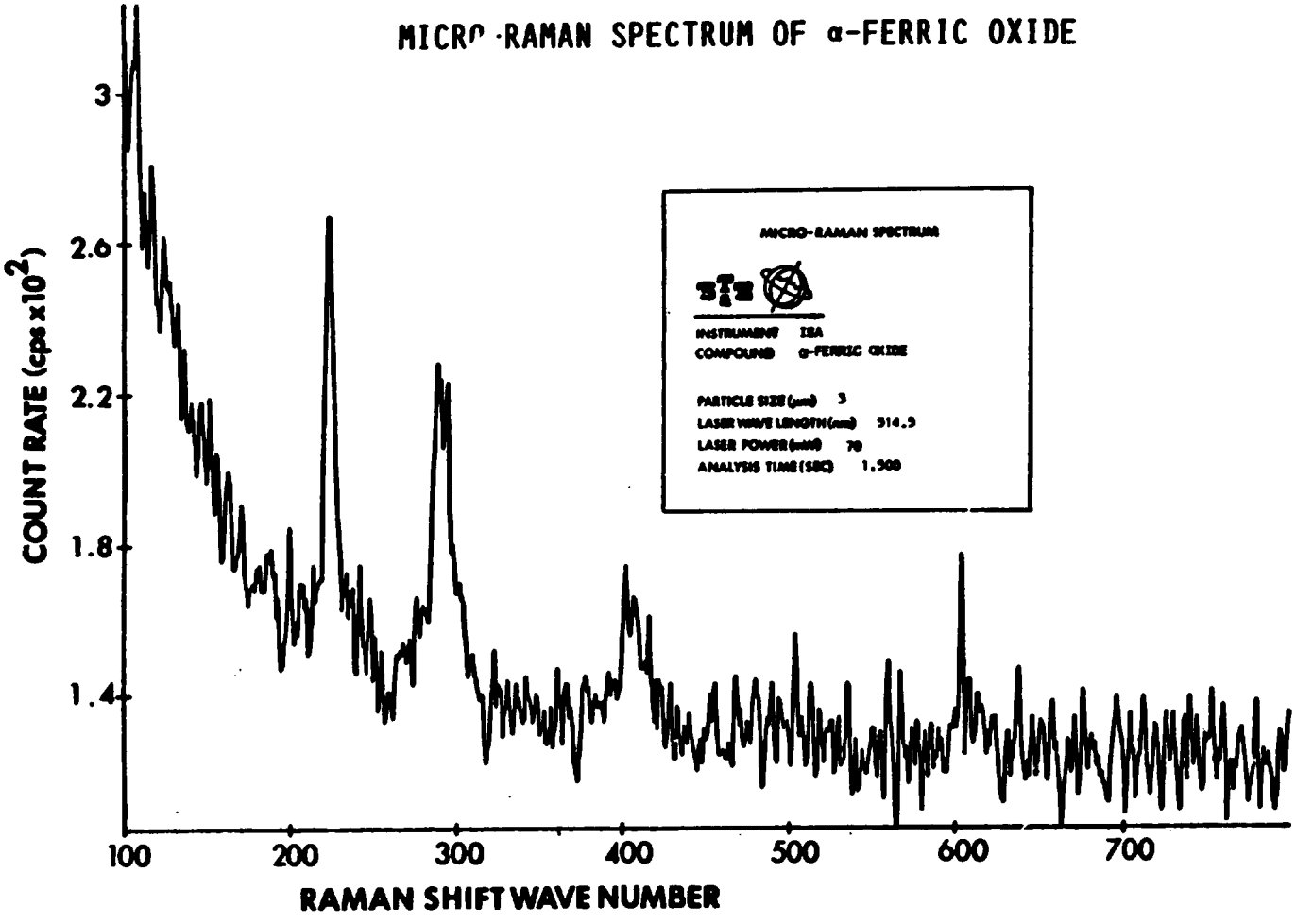
MICRO-RAMAN SPECTRUM OF α-FERRIC OXIDE
COUNT RATE (cps x10²)
3
2.6
2.2
1.8
1.4
100
200
300
400
500
600
700
RAMAN SHIFT WAVE NUMBER
MICRO-RAMAN SPECTRUM
INSTRUMENT IBA
COMPOUND α-FERRIC OXIDE
PARTICLE SIZE (μm) 5
LASER WAVE LENGTH (nm) 514.5
LASER POWER (mW) 70
ANALYSIS TIME (SEC) 1,500

Figure 16:

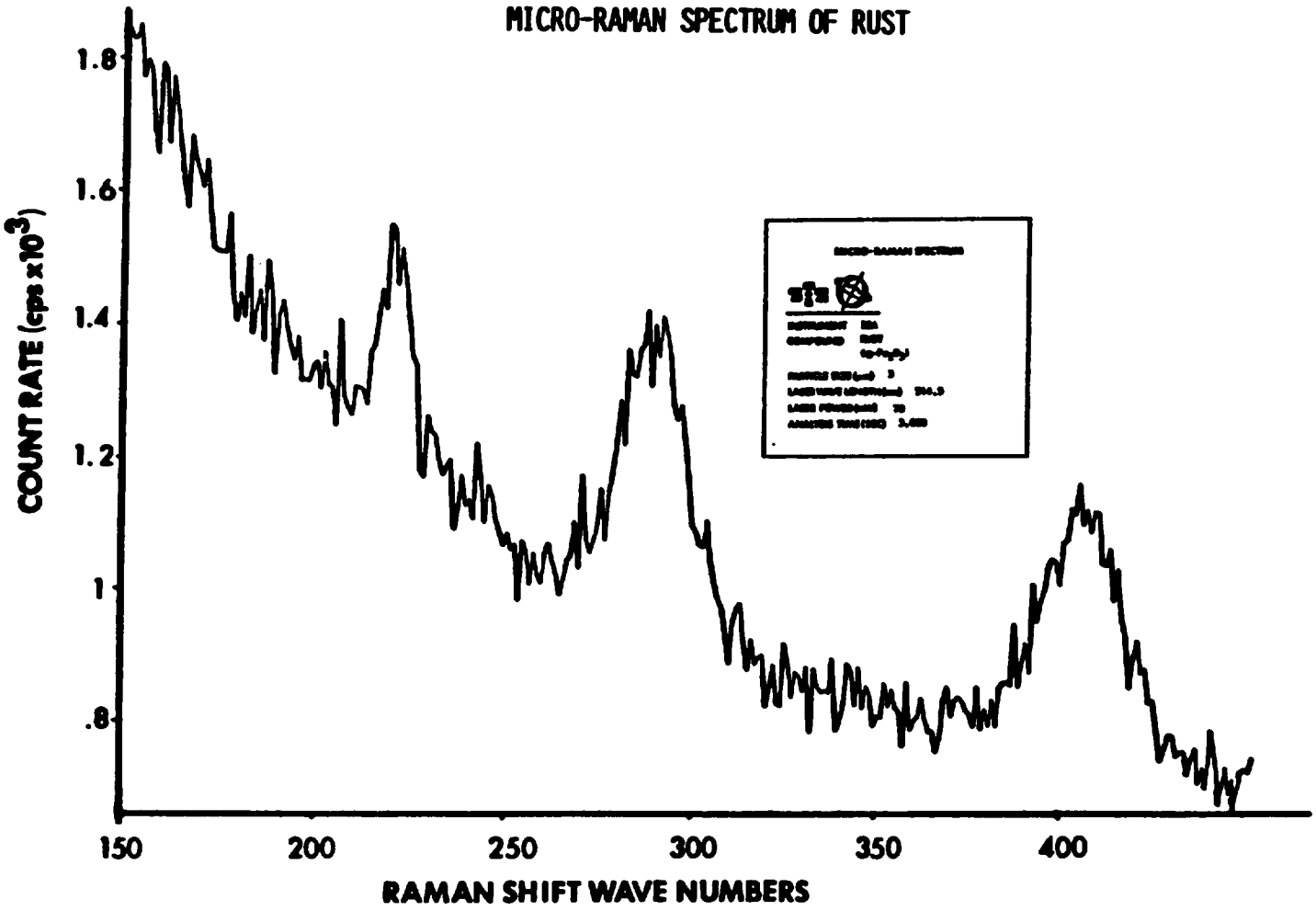
MICRO-RAMAN SPECTRUM OF RUST
COUNT RATE (cps x 10^3)
1.8
1.6
1.4
1.2
1
.8
150
200
250
300
350
400
RAMAN SHIFT WAVE NUMBERS

Figure 17:

micro-Raman spectrum for a rust particle shows distinct peaks at 226 cm^{-1}, 293 cm^{-1}, 298 cm^{-1} and 413 cm^{-1}. From this input, and because of the lack of other spectral lines, it can be concluded that the rust particle is essentially α-Fe_2O_3.

Table 4.1

The Raman Shifts (cm^{-1}) for M_2O_3 Type Crystals

Compound / Transition*	A_{1g}	E_g	E_g	E_g	E_g	A_{1g}	E_g
Al_2O_3	418	378	432	451	578	645	751
Cr_2O_3	303	-	351	397	530	551	609
Fe_2O_3	226	245	293	298	413	500	612

*A_{1g} = Symmetric Stretch

E_g = Asymmetric Stretch and Bend

Figure 18 is due to SiO_2. This is a difficult spectrum to obtain in micro-Raman because of its small Raman cross section [10].

Table 4.2 summarizes the Raman shifts for α-quartz (α-SiO_2). Although the information contained in this table is primarily used for structural information, it does have application in the identification of compounds in mixtures because it permits the selection of spectral lines which are in a clear region on the spectral ramp, thus avoiding ambiguities. The spectral lines in Figure 18 are difficult to assign because of the poor spectral resolution. The strong line at 466 cm^{-1} is the only one that can be positively identified.

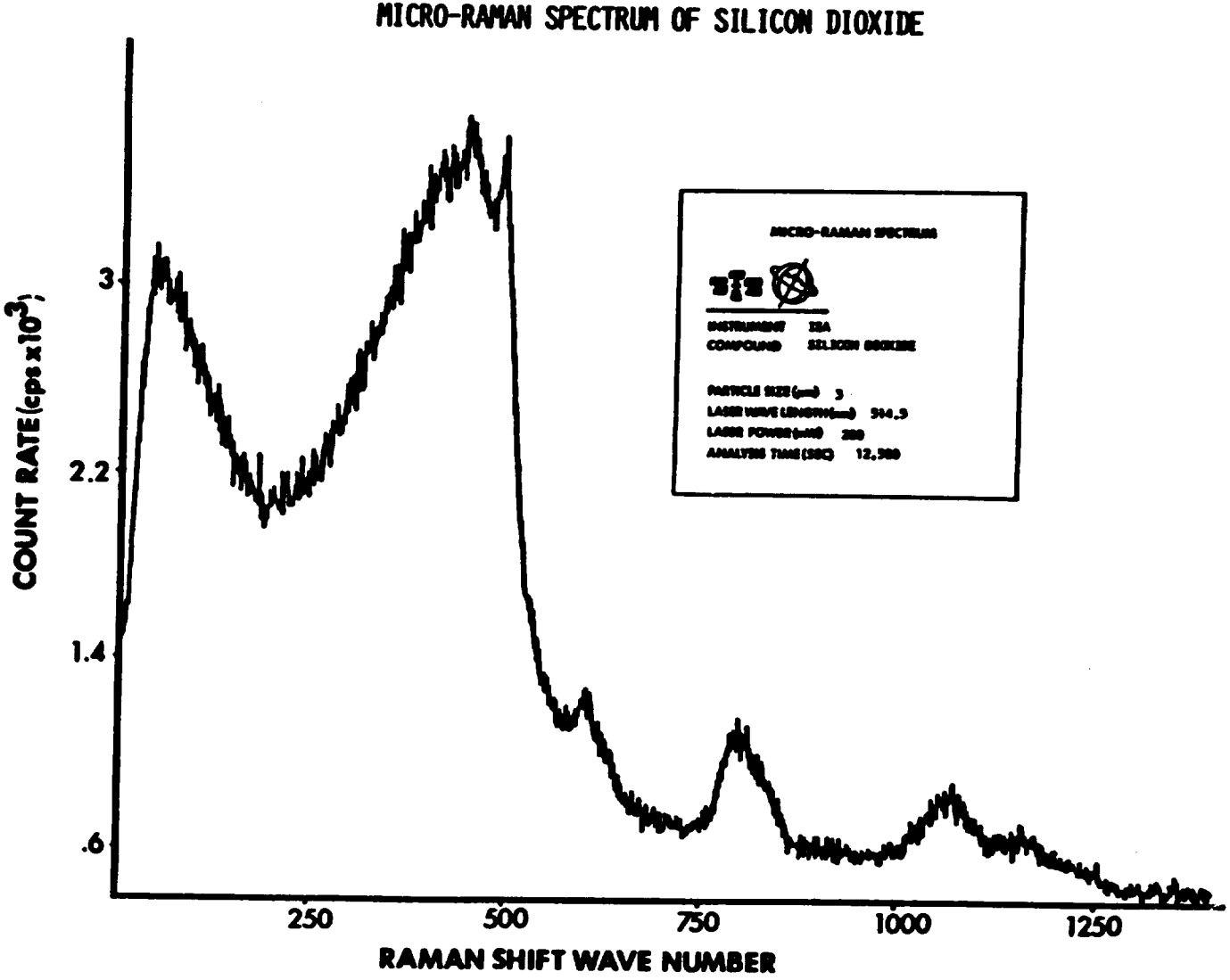
MICRO-RAMAN SPECTRUM OF SILICON DIOXIDE
COUNT RATE (cps x 10³)
3
2.2
1.4
.6
250
500
750
1000
1250
RAMAN SHIFT WAVE NUMBER
MICRO-RAMAN SPECTRUM
INSTRUMENT 32A
COMPOUND SILICON DIOXIDE
PARTICLE SIZE (μm) 3
LASER WAVE LENGTH (nm) 514.5
LASER POWER (mW) 200
ANALYSIS TIME (SEC) 12,300

Figure 18:

Table 4.2

The Raman Shifts (cm^{-1}) for α-SiO_2 [10,11]

Compound / Transition*	A_1	E_L	E_T	E_{L+T}
α-SiO_2	147	403	394	128
	207	508	452	264
	355	811	798	698
	466	1233	1067	1161
	1081			

*A_1 = Symmetric Stretch

E_L = Asymmetric Stretch and Bend Longitudinal Polarization

E_T = Asymmetric Stretch and Bend Transverse Polarization

E_{L+T} = Asymmetric Stretch and Bend Longitudinal and Transverse Polarization

Figure 19 is the micro-Raman spectrum of PbO_2. The peak at 145 cm^{-1} is the low frequency symmetric stretch. Excellent signal to noise is obtained with 10 mW of 514.5 nm laser power and a 1,225 s analysis time for a 3 μm particle.

Figure 20 is a demonstration of micro-Raman's ability to measure organic compounds. Kevlar was chosen because of previous experience with this material and because it has a high fluorescence background which makes it difficult to measure. The spectrum shown was taken on the ISA system using a 3 μm particle, 40 mW of 514.5 nm laser power and a 550 s analysis time. All of the peaks necessary to "fingerprint" the molecule are identifiable even though they are superimposed on a broad band fluorescence. Using a system which has a smaller laser spot, requires less irradiation power and shorter analysis times would

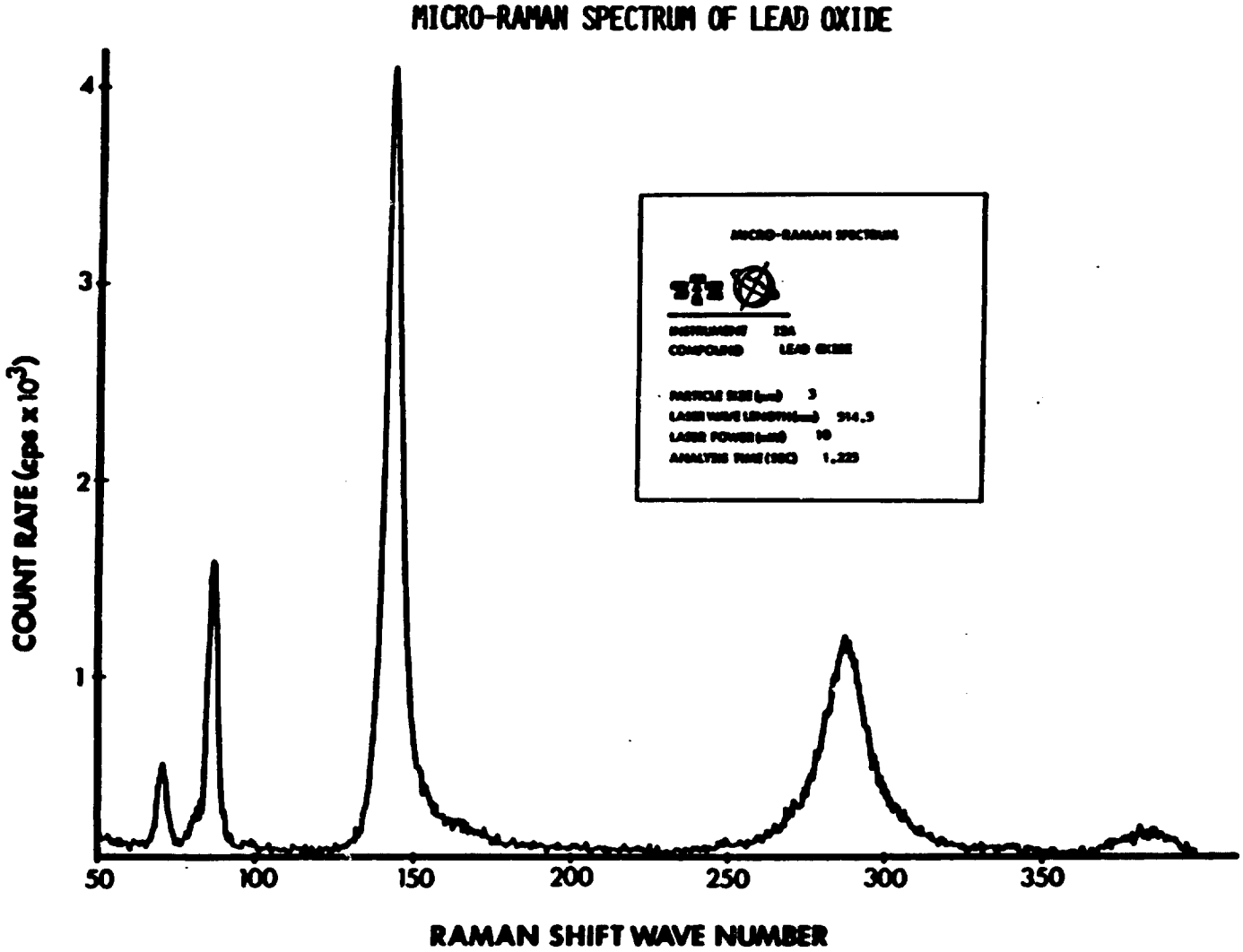
MICRO-RAMAN SPECTRUM OF LEAD OXIDE
COUNT RATE (cps x 10³)
4
3
2
1
50
100
150
200
250
300
350
RAMAN SHIFT WAVE NUMBER
MICRO-RAMAN SPECTRUM
INSTRUMENT
COMPOUND
LEAD OXIDE
PARTICLE SIZE (μm) 3
LASER WAVE LENGTH (nm) 514.5
LASER POWER (mW) 10
ANALYSIS TIME (SEC) 1.225

Figure 19:

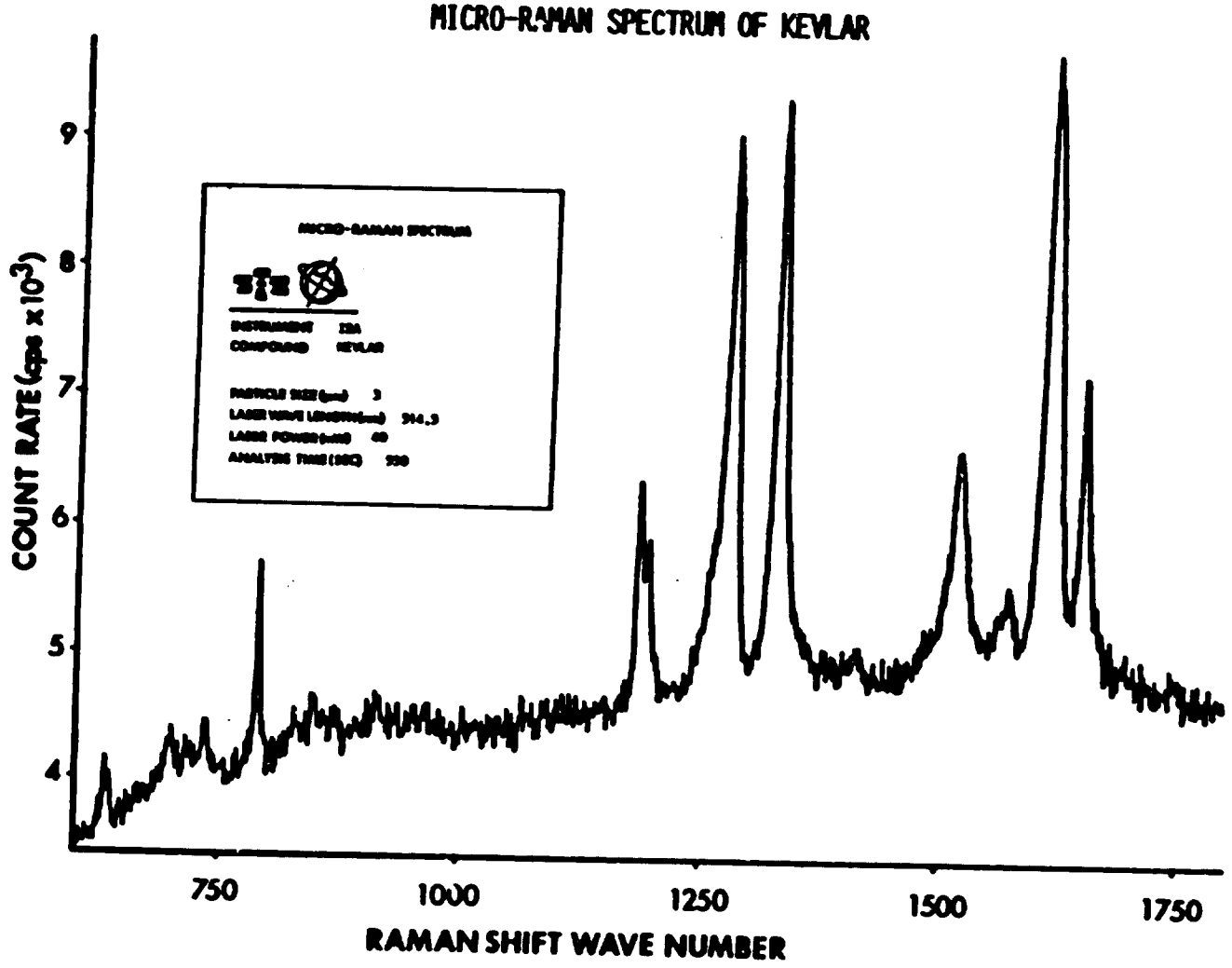
MICRO-RAMAN SPECTRUM OF KEVLAR
COUNT RATE (cps x 10³)
9
8
7
6
5
4
750
1000
1250
1500
1750
RAMAN SHIFT WAVE NUMBER
MICRO-RAMAN SPECTRUM
INSTRUMENT
COMPOUND KEVLAR
PARTICLE SIZE (μm) 3
LASER WAVE LENGTH (nm) 514.5
LASER POWER (mW) 40
ANALYSIS TIME (SEC) 200

Figure 20:

greatly increase the quality of the data.

In Figure 21 the problem with fluorescence backgrounds is further emphasized. Although several strong spectral lines are still obvious, the signal to noise is poor and there is no assurance that some spectral information has not been hidden. Here again, smaller spot size would help considerably (look at only restricted areas of sample) as would less laser power and reduced observation times.

In Figures 22 and 23 the micro-Raman spectra for two minerals are shown. Figure 22 is for hematite. This is composed of Fe_2O_3 and as expected from Table 4.1, the micro-Raman lines at 226 cm^{-1}, 245 cm^{-1}, 293 cm^{-1}, 298 cm^{-1} and 413 cm^{-1} are easily discernible. In cases such as this, where the material of interest is both thermally and photo stable the long analysis times and high power can be tolerated. In Figure 23 (the only acceptable spectra from the SPEX instrument using micrometer particles) the micro-Raman spectra for the framework silicates microcline and low albite are shown. The spectral lines at 288 cm^{-1}, 496 cm^{-1} and 506 cm^{-1} can be identified with the tetrahedral Si-O configuration. In theory, microcline and low albite should have similar lines except for a very small shift due to the differences in size and molecular weight between K and Na. The microcline spectrum, however, shows an additional line at 413 cm^{-1}. This probably is due to the presence of a disorder in the microcline and may be usable in diagnosing particle history.

Figure 24 is an unknown supplied by NASA-Langley. Here the particle was measured directly on the collector (impactor) substrate. The broad band fluorescence is probably due to the visually observable oily film on the substrate. This background could be greatly reduced, and in fact eliminated, if the laser spot size was smaller than 1.0 μm rather than larger than 2.0 μm the size of the aerosol. In addition, heating the sample to remove the volatiles would help. Although there is little data content in the existing spectrum, based on

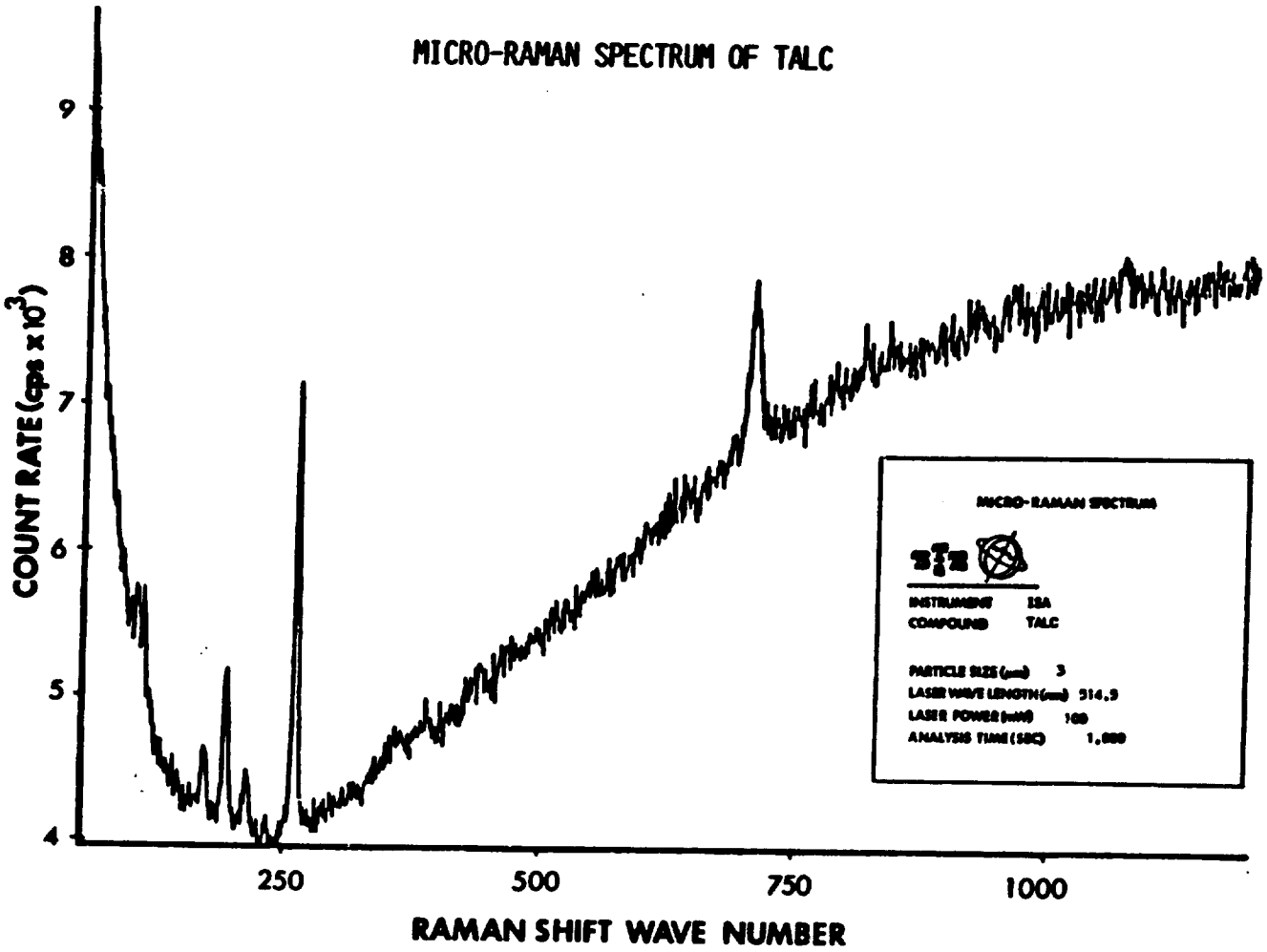
MICRO-RAMAN SPECTRUM OF TALC
COUNT RATE (cps x 10³)
9
8
7
6
5
4
250
500
750
1000
RAMAN SHIFT WAVE NUMBER
MICRO-RAMAN SPECTRUM
INSTRUMENT 18A
COMPOUND TALC
PARTICLE SIZE (μm) 3
LASER WAVE LENGTH (nm) 514.5
LASER POWER (mW) 100
ANALYSIS TIME (SEC) 1,000

Figure 21:

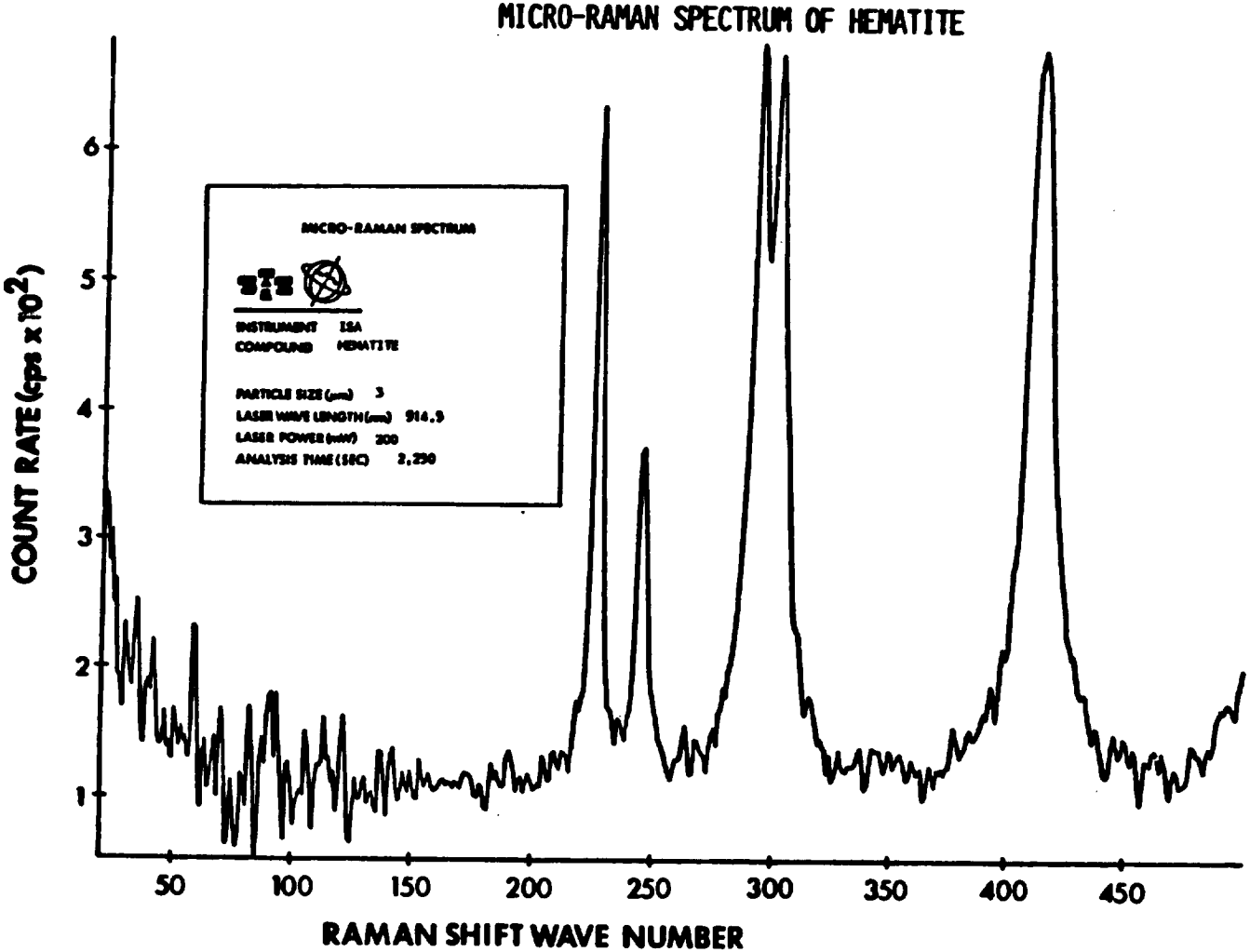
MICRO-RAMAN SPECTRUM OF HEMATITE
COUNT RATE (cps x 10²)
RAMAN SHIFT WAVE NUMBER
MICRO-RAMAN SPECTRUM
INSTRUMENT ISA
COMPOUND HEMATITE
PARTICLE SIZE (μm) 3
LASER WAVE LENGTH (nm) 514.5
LASER POWER (mW) 200
ANALYSIS TIME (SEC) 2,250

Figure 22:

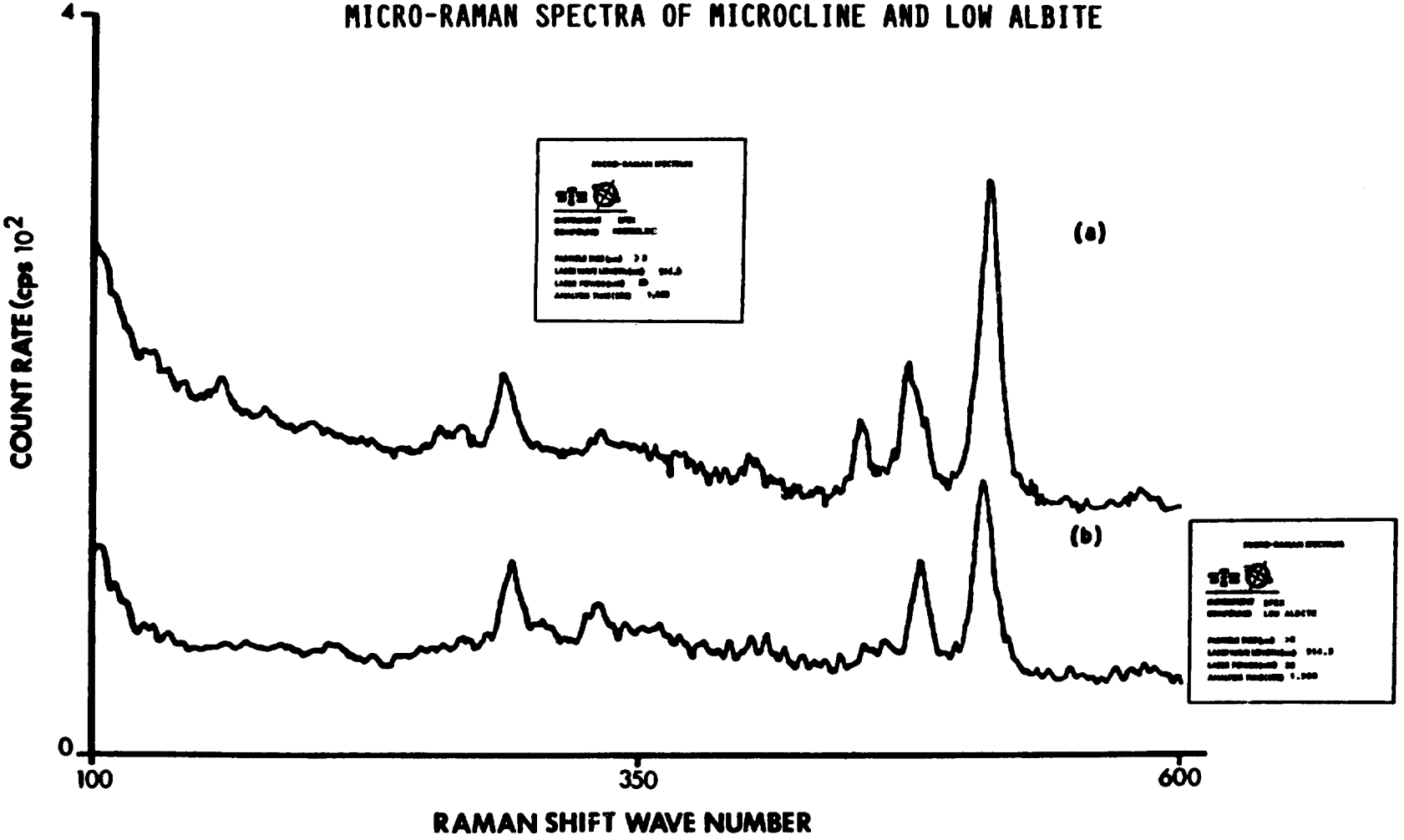
MICRO-RAMAN SPECTRA OF MICROCLINE AND LOW ALBITE
COUNT RATE (cps 10²)
4
0
(a)
(b)
100
350
600
RAMAN SHIFT WAVE NUMBER

Figure 23:

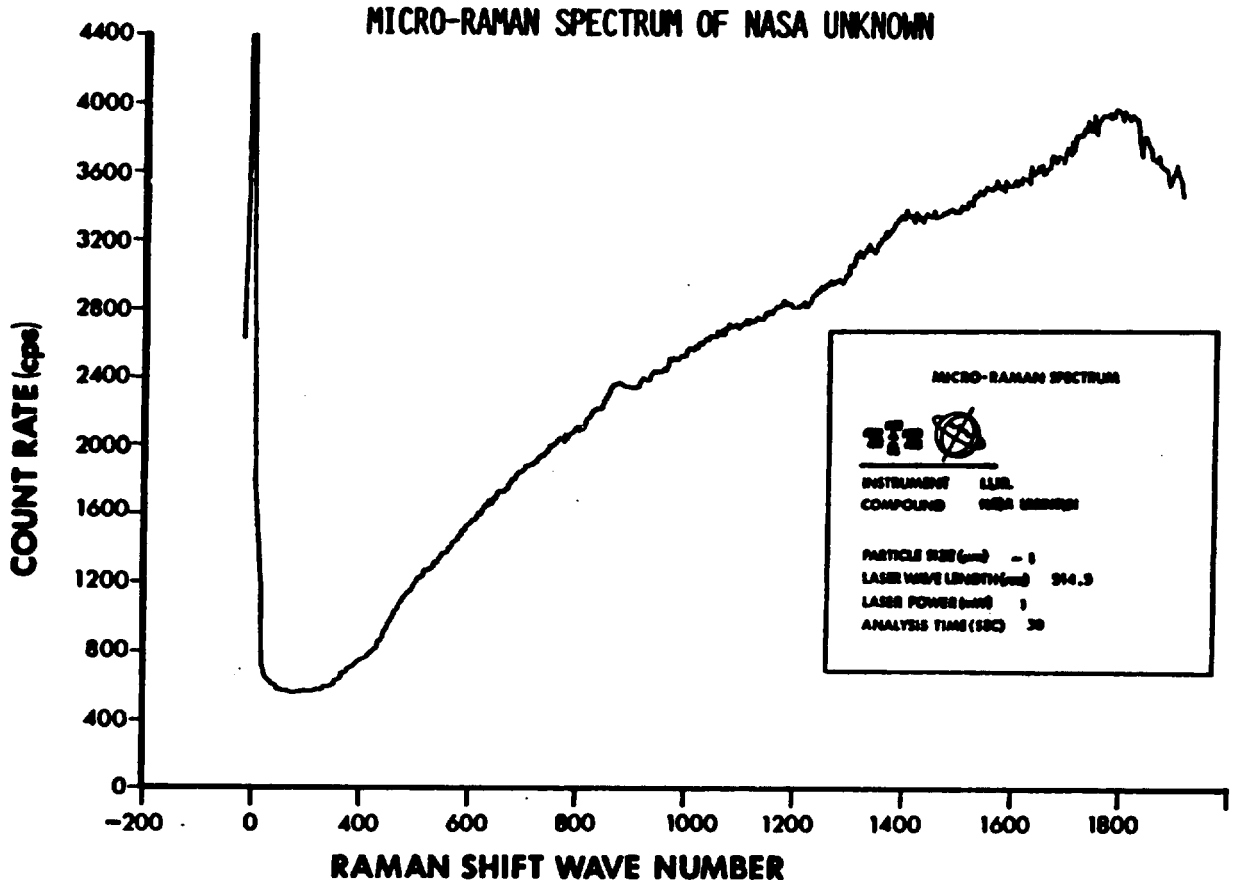
MICRO-RAMAN SPECTRUM OF NASA UNKNOWN
COUNT RATE (cps)
4400
4000
3600
3200
2800
2400
2000
1600
1200
800
400
0
-200
0
400
600
800
1000
1200
1400
1600
1800
RAMAN SHIFT WAVE NUMBER
MICRO-RAMAN SPECTRUM
INSTRUMENT
COMPOUND
LASER WAVE LENGTH(nm) 514.5
LASER POWER(mW) 1
ANALYSIS TIME(SEC) 30

Figure 24:

the extant spectra, and calculations for the performance of the next-generation micro-Raman spectrometer a very high confidence exists that collected aerosols greater than 0.3 μm in diameter will be able to be routinely identified and quantified while particles from 0.1 μm to 0.3 μm should be analysable with a minimum operator effort. A skilled spectroscopist may even be able to measure selected particles below 0.1 μm.

5.0 Practical Considerations in Micro-Raman Spectroscopy

In this section the theoretical calculations for a new-generation micro-Raman system are presented. Where possible, actual measured values are used for the input parameters.

5.1 Thermal Considerations

The radiant intensity of Raman scattered light can be expressed as:

$$I_R = (\partial\sigma/\partial\Omega)NI_0 \qquad (1)$$

where:

$\partial\sigma/\partial\Omega$ = the total Raman cross section (cm^2/steradian molecule);

N = the number of like molecules in the scattering volume;

I_R = the Raman scattered intensity (watts/steradian);

I_0 = the incident laser intensity (watts/cm^2).

In principle, equation (1) indicates that the Raman intensity is directly proportional to the incident laser intensity. This would imply that Raman information can be obtained from the smallest of particles simply by increasing the incident intensity. This is a simplification that fails in micro-Raman due to particle heating effects. For example, a 1-mW laser focused to a 1-micron diameter represents an intensity of 127 kw/cm^2. An isolated (thermal insulated) particle of absorption coefficient of 0.1 cm^{-1} exposed to this intensity will experience a temperature rise of 80°C/s.

$$\Delta T = Q/mC \qquad (2)$$

where:

ΔT = temperature rise per unit time (°C/s);

Q = energy absorbed (J/s) ;

m = sample mass (gm);

C = specific heat capacity (J/g°C).

This temperature rise (80°C/s) would vaporize most microparticles in a matter of seconds.

Fortunately, it is possible to protect a particle from this fate by proper heat sinking. This can be accomplished by attaching the particle either directly, or through a thermal contact medium, to a substrate of high thermal conductivity. Figure (25) shows the thermal transfer geometry diagrammatically. It is possible to predict the temperature rise of a particle as a function of incident intensity subject to the following assumptions: (i) Fourier's Law is valid, (ii) steady state is achieved and (iii) T_0 can be maintained constant.

Under these constraints the thermal transfer reduces to:

$$q = I_0 \alpha_s \ell_s \tag{3}$$

where:

q = the energy (heat) flux/unit area into sample (j/s cm^2);

α_s = the sample absorption coefficient;

ℓ_s = the absorption length (sample thickness).

Applying Fourier's Law and steady state:

$$q = k_s/\ell_s \ (T_s - T_c) \tag{4}$$

or

$$q = k_c/\ell_c \ (T_c - T_0) \tag{5}$$

which yields a temperature rise of:

$$\Delta T = T_s - T_0 \tag{6}$$

or

$$\Delta T = [(\ell_s/k_s) + (\ell_c/k_c)] \ I_0 \alpha_s \ell_s \tag{7}$$

Equation (7) makes it possible to predict the temperature rise providing a few fundamental parameters (particle size, absorption coefficient, thermal conductivity, laser intensity, and thermal contact conductivity) are known. If the particle is directly attached to the substrate, equation (7)

THERMAL TRANSFER GEOMETRY

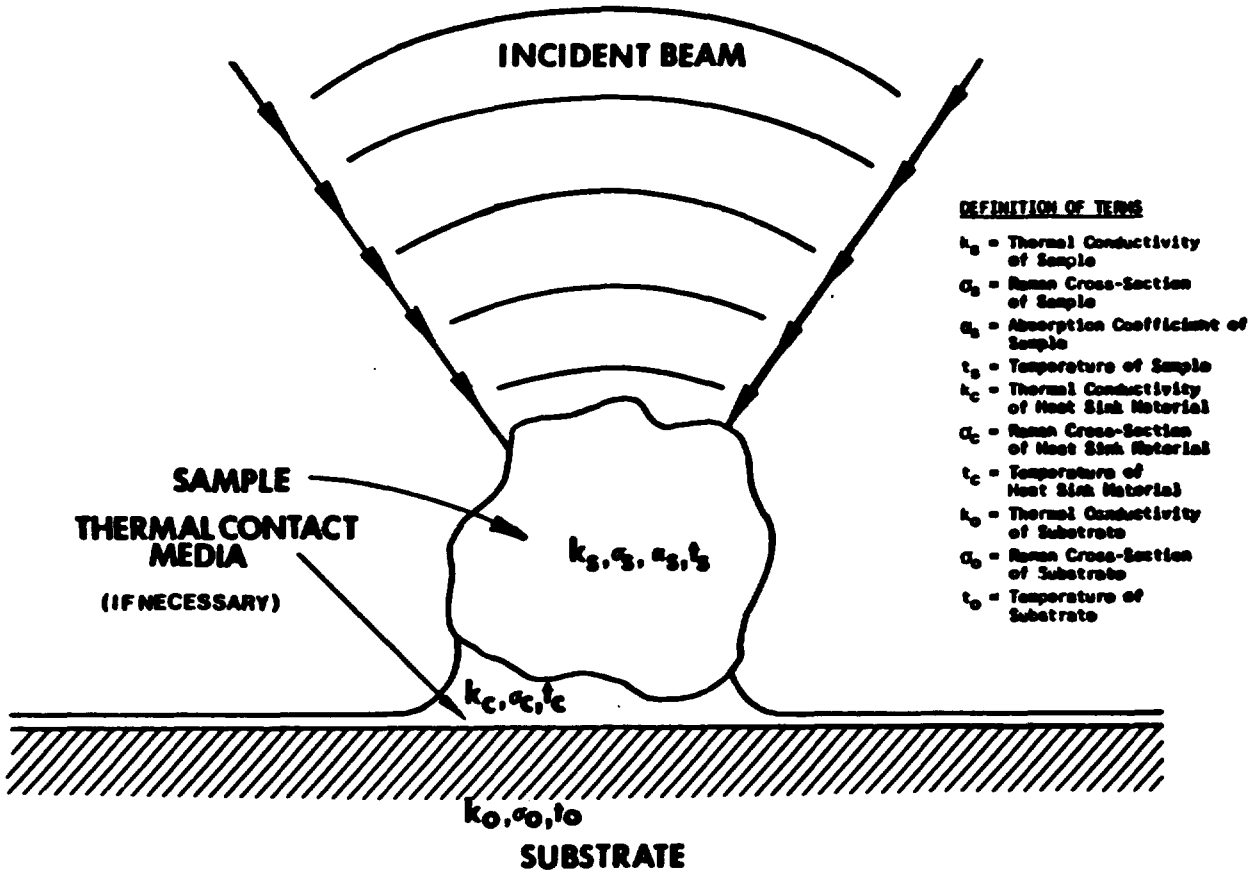

Figure 25:

reduces to:

$$\Delta T = (\ell_s/k_s)\, I_o \alpha_s \ell_s \qquad (8)$$

5.2 Signal Strength

The calculations performed above give a relation by which the maximum laser intensity to which a particle can be exposed can be estimated. This then gives the ability to predict the maximum Raman signal (watts/steradian) that will be scattered by the sample. As an example, the Raman signal generated by a moderately absorbing 0.3 μm-diameter particle with an average Raman cross section (for solids) can be calculated.

From equation (1):

$$I_s = (\partial\sigma/\partial\Omega) N I_o \qquad (9)$$

where:

I_s = intensity of Raman scattered light from the sample (watts/steradian);

N = number of sample particles

$= 4/3\pi r^3 (N_o \rho/M)$;

where:

N_o = Avogadro's Constant ($6.02 \cdot 10^{23}$ mol^{-1});

M = sample molecular weight;

ρ = sample density (g/cm^3);

r = particle radius (cm).

If, for example, the following realistic values are substituted into equation (9):

I_o = 1 MW/cm^2 (0.7 mW focused to 0.3 μm);

r = $0.15 \cdot 10^{-4}$ cm;

ρ = 3 g/cm^3;

M = 100;

$\partial\sigma/\partial\Omega$ = 10^{-30} $cm^2/sr\ mol$;

then

$$N = 2.5 \cdot 10^{8} \text{ particles}$$

and finally,

$$I_S = 2.5 \cdot 10^{-14} \text{ watts/sr}$$

or, in terms of photons:

$$P_S = I_S / E_S \tag{10}$$

where:

E_S = the energy of a single photon (J);

= hc/λ

where:

h = Planck's Constant ($6.63 \cdot 10^{-34}$ J/s);

c = speed of light ($3 \cdot 10^{10}$ cm/s);

λ = wavelength of scattered photon ($5 \cdot 10^{-5}$ cm).

Then substitution into equation (10) yields:

$$E_S = I_S \lambda / hc \tag{11}$$

and substituting the above values:

$$E_S = 4 \cdot 10^{-19} \text{ J}$$

and

$$P_S = 6.3 \cdot 10^{4} \text{ photons/sec sr}$$

5.3 Instrument Efficiency

The order of magnitude calculations made in the previous section indicates a more than adequate Raman scattered signal intensity from a representative sample. This signal, however, must subsequently be collected and measured. By definition, this can only be done with equipment that has less than 100% throughout. Optimizing throughput is essential for submicron Raman analyses and is one of the key objectives of this research effort. It is possible to estimate, with significant accuracy, the throughout of the individual components under consideration. These will include a collection objective,

wavelength dispersing monochromators, stray light rejecting filters, and a quantum detector.

The efficiency can be represented as:

$$\eta_E = \Omega_C \eta_F \eta_S \eta_D \qquad (12)$$

where:

Ω_C = solid angle collected (sr);

η_F = efficiency of prefilter;

η_S = efficiency of spectrograph;

η_D = detector quantum efficiency (counts/photon).

For example:

Ω_C = 0.8 sr for an f/1 collection lens;

η_F = 0.55 for a double grating prefilter with enhanced surfaces;

η_S = 0.7 for a single grating, single mirror spectrograph;

η_D = 0.1 for a diode array optimized at 500 nm.

Substitution of the above values into equation (12) gives:

$$\eta_E = 0.03$$

The ultimate system efficiency will depend on the final design of the optical system and the actual components selected. This will not vary much from this calculation. It is, therefore, valid to use this efficiency for the illustrative examples that follow.

5.4 Background Signals

Calculations in the previous two sections indicate that a representative 0.3 micron diameter sample will yield an actual signal rate of

$$P_C = P_S \eta_E \qquad (13)$$

and substitution of previous calculated values for P_S and η_E gives:

$$P_C = 1.9 \cdot 10^3 \text{ counts/s}$$

The remaining step of this feasibility analysis is then to determine if this signal level provides acceptable signal to noise (S/N) after all sources

of background are considered. This requires identifying the background sources and estimating their strength.

The three primary sources of background are fluorescence (both sample and impurity); stray light (elastic scattered light collected by the detector system); and detector dark noise (no signal on the detector).

Fluorescence intensities will be almost as varied as sample types. Some samples will have intrinsic fluorescence or impurity fluorescence of sufficient strength to completely obscure the Raman signals, while other samples will have no fluorescence. The vast majority of samples will be somewhere in between. It is impractical to give anything but a representative calculation based on experience in the laboratory.

The photon flux represented from the incident laser power (0.7 mw) is:

$$N_p = P_o/E_o \tag{14}$$

where:

N_p = the photon flux from the initial laser power (photons/s);

P_o = the initial laser power;

E_o = the energy of a photon at the laser wavelength

= hc/λ_o (see equation 10).

If:

P_o = 0.7 mW;

λ_o = 488.0 nm ($4.88 \cdot 10^{-5}$ cm);

then

$$N_p = 1.73 \cdot 10^{15} \text{ photons/s}$$

Considering that the sample volume contains only ~10^8 molecules, this photon flux will almost always saturate fluorescence transitions. As a result, the fluorescence yield of the sample is a function of the number of potential fluorescence scatters. The lifetime of the fluorescence, τ (a measure of how

fast the molecule can be cycled through the ground state), and the fluorescence quantum yield Q_f (the ratio of fluorescence light quanta to incident light quanta). This can be expressed as:

$$P_f = NQ_f\phi_f\tau^{-1} \quad (15)$$

where:

P_f = signal rate from the fluorescence (photons/s);

N = the number of sample particles;

Q_f = the fluorescence quantum efficiency;

ϕ_f = the fraction of the sample that is fluorescent;

τ = fluorescence lifetime.

If the assumption is made that:

ϕ_f = 1 ppm (10^{-6});

Q_f = 10%;

τ = 10^{-5} s;

then:

$$P_f = 2.5 \cdot 10^6 \text{ photons/s}$$

This is a seemingly overwhelming number until it is remembered that this fluorescence is generally spread in wavelength throughout much of the visible spectrum. If, for example, this range is represented by 3000 cm^{-1} and the detector will view the signal in units (channels) of 2 cm^{-1}, then P_f reduces to:

$$P_f = 1.7 \cdot 10^3 \text{ photons/s}$$

Further correcting for system efficiency (0.03) reduces the fluorescence contribution to:

$$P_f = 50 \text{ counts/s}$$

This is well under the Raman count rate of almost 2,000 counts/s.

The stray light, P_E, observed by the detector can be calculated to a

higher degree of accuracy. If it is assumed that the particle is moderately opaque then it will elastically scatter approximately 10% of the incident light (a perfect dielectric sphere will scatter 40% of the incident light). If it is further assumed that half is scattered into the hemisphere containing the collection lens then the amount reaching the spectrometer is the ratio of the collection solid angle to 2π. Thus:

$$N_E = N_p \psi (\Omega_C / 2\pi) \tag{16}$$

where:

N_E = the photon flux from the elastic scattering (photons/s);

ψ = portion of incident light elastically scattered.

Substituting:

N_p = $1.73 \cdot 10^{15}$ (from previous calculations);

ψ = 0.1;

Ω_C = 0.8 (see previous discussion).

Then:

$$N_E = 2.2 \cdot 10^{13} \text{ photons/s}$$

Modern multiple grating spectrometers have stray light rejections of approximately 10^{-11}; therefore, the detector will see 220 photons/s. With an efficiency of 0.1 the resulting signal from elastic scattering is:

$$N_E = 22 \text{ counts/s.}$$

The detector of choice will be an optical multichannel device (OMA) [either a silicon intensified target (SIT) or a diode array (DAR)] because of their high versatility and good sensitivity. These detectors are operated cooled and have manufacturers' dark noise , P_D, specifications of from 2 to 5 dark counts/channel. The authors of this report have operated a SIT for the past 4 years. Experience is 2-4 dark counts/channel at -57°C. For the purpose of this feasibility calculation we will take the worst case of 5 counts/channel.

To summarize the calculations:

Raman Signal: P_C = 1,900 counts/s

Fluorescence: P_F = 50 counts/s channel

Stray Light: P_E = 22 counts/s channel

Dark Noise: P_D = 5 counts/s channel

In the previous calculations it was convenient to describe the background as a contribution to a resolution element (channel of an OMA). However, the Raman signal strength was computed on a total cross-section (integrated signal over the Lorentzian lineshape). Typically, Raman transitions are 2 to 20 cm^{-1} in width. If it is assumed that a transition 10 cm^{-1} in width is being observed with a spectrograph resolution of 2 cm^{-1}/channel, the Raman signal (P_C) approximately reduces to 380 counts/s channel. With the background totaling 77 counts/s channel, the signal to background (S/B) is 5.

This is a very encouraging result since the estimates were based on a moderate Raman scattering cross-section (the 992 cm^{-1} line of benzene is 27 times as strong as the example) and the choice of background situations was slightly to the pessimistic side.

This feasibility exercise was used to guide our preliminary design of a submicron Raman spectrometer. Preliminary information about this instrument is contained in Section 6 of this report. More specific details are contained in the SBIR Phase II proposal (Solicitation No. 84-1-II).

6.0 Preliminary Design

It is now possible, based on the results presented in Sections 4 and 5, to construct a preliminary design of a micro-Raman spectrometer that meets the objectives of this research effort. Figure (26) is a block diagram of the proposed instrument. The excitation source will be an Ar-Ion laser with numerous available transitions in the visible and capable of computer control. The illuminator will be of an innovative design that will use the coherent and monochromatic nature of several like-laser beams to produce a less than diffraction-limited excitation spot size. The sample stage will be computer controlled and incorporated in an optical scanning microscope. This will provide optical resolution of the sample to 0.3 μm and computer mapping of an entire sample substrate. Preselection of those particles of interest will be accomplished by a modified "pattern recognition" routine. All operator interactions will be through a computer terminal and all viewing of sample and data will be by CRT. Raman signals will be collected by a microscope objective and directed through a prefilter (to remove elastically scattered light) and into a spectrograph. The signal will be measured on an optical multichannel analyzer that will have an optional stand-alone capability (its own keyboard, CRT, torage, etc). The data will be stored on disk and magnetic tape and presented in hard copy. The computer will be able to do all basic routines such as background subtract; add, subtract, divide, and multiply spectra; and spectral correlation. ST&E considers the design details for this new-generation micro-Raman spectrometer to be a "trade secret" and "proprietory" in nature. To permit free dissemination of this document and to protect its interests, ST&E will put the detailed design in its Phase II proposal.

BLOCK DIAGRAM OF NEXT GENERATION MICRO-RAMAN SPECTROMETER

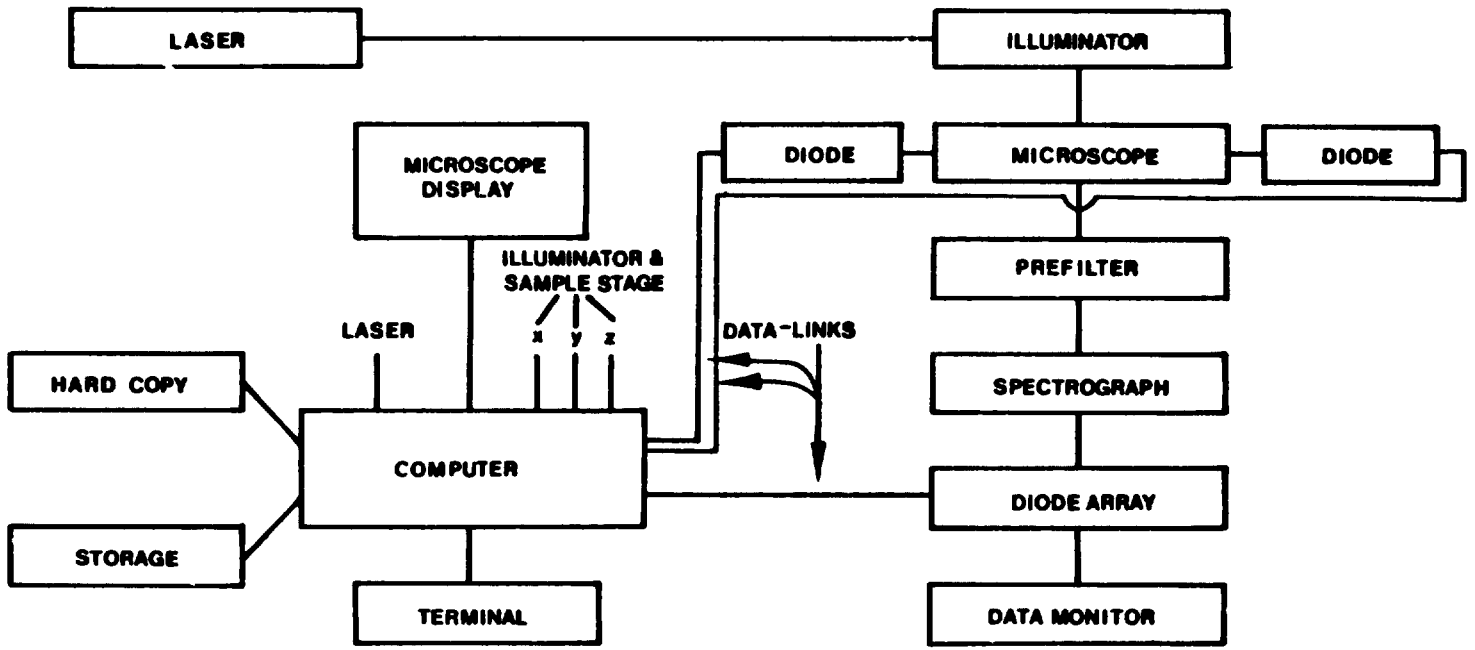

Figure 26:

7.0 References

[1] Ishida, H.; and Ishitani, A.; "Raman Microprobe Analysis of Thin Films formed on the Surface of Silver Electrical Contacts Utilizing the Surface-enhanced Raman Scattering Effects"; App. Spec., 37, 450, (1983).

[2] Irish, D. E.; and Chen, H.; "The Application of Raman Spectroscopy to Chemical Analysis"; App. Spec., 25, 1, (1971).

[3] Frass, L. M.; Moore, J. E.; and Salzberg, J. B.; Raman Characterization Studies of Synthetic and Natural $MgAl_2O_4$ Crystal"; private communication, (1978).

[4] Vidano, R.; and Fischbach, D. B.; "New Lines in the Raman Spectra of Carbons and Graphite"; J. Am. Ceramic Soc., 61, 13, (1978).

[5] Stafford, R. G.; and Chang, R. K.; "Absolute Raman Scattering Cross Sections of Sulfate and Bisulfate and Their Application to Aqueous Aerosol Monitoring"; presented at the National Bureau of Standards Eigth Materials Research Symposium on Methods and Standards for Environmental Measurements, Gaithersburg, MD, (1976).

[6] Rosen, H.; and Novakov, T.; "Chemical Characterization of Atmospheric Aerosol Particles Using Raman Spectroscopy"; Lawrence Berkeley Laboratory, University of California, Report LBL-5912, (1977).

[7] Michel, D.; Perez, Y. J.; and Collongues, R.; "Study by Raman Spectroscopy of Order-Disorder Phenomena Occurring in Some Binary Oxides with Fluorite-Related Structures"; J. Raman Spec., 5, 163, (1976).

[8] Shussshichinskii, M. M.; "Raman Spectra of Molecules and Crystals"; Chapter 12; Israel Program for Scientific Translations, Kete, Inc.; New York, (1972).

[9] Anderson, A., Editor; "The Raman Effect"; Volume 2: Applications; Chapter 11; Marcel Dekker, Inc., New York, (1973).

[10] Galeener, F. L.; Mikkelsen, J. C., Jr.; Geils, R. H.; and Mosby, W. J.; "The Relative Raman Cross Sections of Vitreous SiO_2, GeO_2, B_2O_3, and P_2O_5, Appl. Phys. Lett., 32, (1978).

[11] Briggs, R. J.; and Ramdas, A. K.; "Piezospectroscopy of the Raman Spectrum of α-Quartz"; Phys. Rev. B, 16, 3815, (1977).